

California Polytechnic State University, San Luis Obispo

DigitalCommons@CalPoly

Biomedical Engineering: Graduate Reports and
Projects

Graduate Reports and Projects

3-2022

Abbott Lab Instrumentation Validation

Brandon James Mukai

California Polytechnic State University, San Luis Obispo, mukaibrandon5@gmail.com

Bosung Josh Kim

California Polytechnic State University, San Luis Obispo, Kimjoshb@gmail.com

Follow this and additional works at: https://digitalcommons.calpoly.edu/bmed_rpt



Part of the [Biomedical Devices and Instrumentation Commons](#)

Mukai, Brandon James and Kim, Bosung Josh, "Abbott Lab Instrumentation Validation" (2022).

Biomedical Engineering: Graduate Reports and Projects. Paper 2.

https://digitalcommons.calpoly.edu/bmed_rpt/2

This Dissertation/Thesis is brought to you for free and open access by the Graduate Reports and Projects at DigitalCommons@CalPoly. It has been accepted for inclusion in Biomedical Engineering: Graduate Reports and Projects by an authorized administrator of DigitalCommons@CalPoly. For more information, please contact digitalcommons@calpoly.edu.

Abbott Lab Instrumentation Validation

Project Report

Brandon Mukai, Bosung Josh Kim

bmukai@calpoly.edu, bkim51@calpoly.edu

Sponsored by Christopher Porterfield MD, MPH, FACC



Table of Contents

Executive Summary	5
Project Background and Context	7
Clinical Relevance	7
Figure 1: Typical placement of cardiac catheters during an electrophysiology study as seen through fluoroscopy	10
Catheters	11
Figure 2: Example of a bipolar electrogram read by 2mm and 10mm spaced electrodes.	12
Figure 3: Voltage mapping of low-voltage substrate causing a reentrant tachycardia.	13
Figure 4: Abbott’s Advisor HD Grid cardiac mapping catheter	14
Figure 5: Voltage maps of the right ventricle using a standard linear catheter and a multielectrode catheter.	15
Figure 6: Abbott’s TactiCath Sensor Enabled cardiac ablation catheter	18
Table 1: Popular Abbott ablation and diagnostic catheters	18
EnSite Precision	23
Figure 7: Placement guide of surface electrode patches, system reference patch, patient reference sensors, defibrillator patch, and RF generator patch relative to the Precision Field Frame	24
Figure 8: Sensor Enabled PrecisionLink (left) and Precision Field Frame (right)	25
Figure 9: Voltage maps of the left atrium and pulmonary veins before RF ablation to isolate the pulmonary veins to treat atrial fibrillation.	25
InVitro System	26
Figure 10. Cazolari’s In-Vitro Experimental Set-up	27
Figure 11. Setup for bench model experiments	28
Saline Solution	29
Cal Poly’s Wet Lab	30
Specification Development	32
Figure 12. Required Components of a Successful System: Diagram to show components that make up a successful functioning wet lab for this project.	33
Concept Generation and Evaluation	37

Figure 13. Flowchart of Concept Iteration: The diagram outlines our methods of concept generation and design of various versions while performing validation testing. [14]	37
Conceptual Models and Analyses	40
The Box Model	40
Figure 14: Concept Sketch of Box Model	40
Hexagon Model	41
Figure 15. Sketch of Hexagon Model Concept	41
Octagon Model (Prototype I)	42
Figure 16. Octagon Model: Physical model of octagon model drying after fabrication.	42
Prototype II	
Figure 17: Prototype II model set for integration testing of the system	43
Final Prototype	43
Figure 18. Final Model Prototype: A) Final Prototype; B) Final Prototype under testing	44
Prototype Manufacturing	45
Figure 19. Tools Used for Manufacturing: A) Table Saw; B) Miter Saw; C) Band Saw	45
Figure 20. Pieces of Acrylic cut in Mustang 60	46
Figure 21. Process of Laser Cutting Acrylic	47
Figure 22. Final Prototype Assembly	47
Prototype Assembly	48
Test Protocol Development	49
Tank Test Protocol	49
Integration Validation Protocol	50
Testing Data and Analyses	54
Table 3: First Prototype Leak Test	54
Table 4: First Prototype Pressure Tests	54
Table 5: Second Prototype Leak Test	56
Table 6: Second Prototype Pressure Tests	56
Table 7: Final Prototype Leak Tests	58
Table 8: Final Prototype Pressure Tests	58
Table 9: Integration Validation Attempts	59
Figure 23: A) Configuration of surface electrode patches, PRS patches, and system reference patch used for integration attempts 1 and 2. B) Configuration of all patches used in integration attempts 3 and 4.	60

Table 10: Study Measurements	64
Discussion and Future Directions	65
References	72
Appendices	77
Appendix A: Hydrostatic Force Calculation	78
Appendix B: Table of Material Properties	79
Table 2: Mechanical Properties of Materials: Acrylic molded, cast, optical sheet, and plexiglass.	79
Appendix C: Detailed drawings and schematics	80
Appendix D: Test data	90
Appendix E: Operation Manuals	95
Protocol for adding EP catheters with RecordConnect	100
Appendix F: Testing Protocol	103
Leak Test Protocol	103
Pressure Test	103
Saline Validation test	103
Appendix G: Manufacturing process instructions	106
Cutting Acrylic	106
Laser Cutting Acrylic	106
Assembly of Acrylic Panes	107
Saline Solution Manufacturing Process	107
Appendix H: Core Customer Charts	109
Appendix I: Penta Chart	112
Appendix J: Gantt Chart	113
Appendix K: Budget	115

Executive Summary

As hospitalizations and deaths due to cardiac arrhythmias constantly remain in several hundreds of thousands annually, it is crucial that the field of electrophysiology continues to advance. Cardiac mapping is an electrophysiology study that is critical for clinicians to diagnose irregular heart rhythms, such as arrhythmias, and treat these diseases. Abbott's EnSite Precision cardiac mapping system serves as an industry leader worldwide for 3D advanced mapping to help diagnose a wide range of arrhythmias. The purpose of our thesis project was to develop a functioning wet lab in Cal Poly's St. Jude research lab that would fully integrate with the EnSite Precision cardiac mapping system for the purpose of future experimentation and demonstration purposes. The EnSite Precision cardiac mapping system is an impedance based mapping system that utilizes a magnetic field to improve stability and allow for the use of Abbott's Sensor Enabled tools. The goal of the project was to design a wet lab that would serve as a physiological representation of a patient undergoing an EP study using this mapping system. The wet lab contained a tank with a cubical working chamber and a rectangular attached off branch chamber that allowed for separation of the left leg patch and also as a way for users to guide catheters to the object of interest that sits in the main chamber. The final prototype passed all of the pressure and leak tests that were required prior to any integration with the system. Due to the lack of appropriate hardware, the study was performed by using the TactiCath SE ablation catheter rather than a diagnostic catheter with multielectrode splines that is designed for data collection. Using this catheter, three dimensional geometric models were created for the wall of a glass bowl, length and width of a rubber object, and the width of the tank's left wall in the EnSite Precision system. The dimensions of the generated models were compared to the actual physical dimensions and resulted in an absolute error of 13.56 mm for the glass bowl, 20.73 and 5.58 mm

error for the rubber object, and a 31 mm error for the wall of the acrylic tank. Though these error values are not perfectly ideal for precise and accurate model creations, there are simple modifications that can be implemented into the wet lab to significantly reduce these values while expanding the functionality of the lab. These include increasing the workable area inside the tank, removing any objects that can insulate the current being emitted by the surface electrodes, and obtaining a catheter pin block for diagnostic catheters. This validation of the integration between the wet lab and the EnSite precision cardiac mapping system serves as a significant step towards developing a fully functional wet lab that future students, faculty, and industry representatives can use for academic and demonstrational purposes.

Project Background and Context

Over the past 40 years, since the initial catheter ablation procedure was completed, cardiac mapping has become an essential part of electrophysiological procedures. Cardiac mapping is an electrophysiological study that allows physicians to analyze the electrical activity of the heart in order to diagnose and treat cardiovascular disease. Institutions like Cal Poly can utilize professional instrumentation systems with an appropriate wet lab to develop new devices and study various phenomena in an in-vitro physiological environment. Cardiac mapping systems used in tandem with catheter ablation procedures are essential to ensuring that the trend of deaths due to cardiovascular disease continues to decline. This project thesis will signify the importance of the development of a wet lab integrated with Abbott's Ensite Precision Cardiac Mapping System for future product development and in-vitro studies.

Clinical Relevance

Cardiovascular disease is annually the leading cause of death in the United States for both men and women, even though the number of deaths per year has been steadily declining over the last 50 years (Weir, 2016). More specifically, cardiac arrhythmias continuously contribute to 200,000-300,000 deaths per year, according to the UCLA School of Medicine (UCLA, 2020). Cardiac arrhythmias occur when there are abnormalities in electrical impulses that result in irregular heartbeats and conduction patterns. Cardiac arrhythmias are classified by their rate and location of origin. Tachycardia refers to a heart rhythm with a rate that exceeds 100 beats per minute and bradycardia refers to a rhythm with a rate below 60 beats per minute. Supraventricular (atrial origin), ventricular (ventricular origin), and bradyarrhythmia (SA node, AV node or His-Purkinje network) classifications are based on the origin of the electrical conduction where the arrhythmia stems from. Supraventricular (SVT) arrhythmias in the form of

atrial fibrillation and atrial flutter result in rapid heart rate caused by chaotic electrical impulses, though the impulses in atrial flutter may be more rhythmic. In both conditions, the irregular heartbeats cause weaker than normal contractions that slow down the blood flow in the atrium. When this happens, the blood pools are now susceptible to coagulation because the platelets of blood aren't moving fast enough to prevent binding. Coagulation of blood in the atria due to atrial fibrillation and flutter can lead to serious complications such as stroke. There are currently 33 million people in the world with AFib with 5 million new cases diagnosed each year leading it to be the most common type of arrhythmia (Morillo, 2017). Patients with AFib are five times more likely to have a stroke, have a five-fold increase in the likelihood of heart failure, and have twice the likelihood of cardiovascular mortality (Oduyayo, 2016). There are four main treatment options for patients with AFib that include medication, lifestyle changes, cardioversion, and catheter ablation. Although medications and lifestyle changes are typical early intervention treatments to help manage symptoms and risk factors, 50% of patients do not tolerate or respond to medications [Baton, 2019]. Cardioversion by external defibrillator is often used to revert the heart rate back to normal sinus rhythm but 50% of patients often revert back to AFib after one year (Schnabel, 2018). Cardiac mapping and catheter ablation is a procedure used to identify and interrupt the pathways of conduction in the atria that are causing the fibrillation. Recent studies have demonstrated that treatment by this procedure has led to an 88% success rate at the 12-month post-procedure mark (Natale, 2014). Other common SVTs that are treated by ablation/pharmacological management are reentrant tachycardias such as atrioventricular nodal (AVNRT), atrioventricular (AVRT) and focal tachycardias such as atrial tachycardia (Stanford, 2019). Reentrant tachycardias are disorders of impulse transmissions that require at least two conduction pathways with different refractory periods and conduction velocities, both pathways

must connect be connected proximally and distally to the atrium and ventricle, and an appropriately timed premature atrial or ventricular contraction (PAC or PVC) that will travel down the accessory pathway since the normal pathway is in refractory (Ferry, 2007). Chronic management of these reentrant tachycardias include catheter ablation of the accessory (or slow) pathway which in most recent studies have demonstrated 90-95% success rates when three-dimensional electroanatomical mapping (EAM) systems are used to help localize sites for ablation (Tedrow, 2020). All these mentioned conditions can be treated by various forms of therapy, but the more chronic and problematic cases have better success rates when treated by catheter ablation assisted by cardiac mapping (Viswanathan, 2016).

One of the more significant benefits of using 3D EAM systems is the reduction of radiation exposure from fluoroscopy for patients and professional staff during electrophysiology procedures (Giaccardi, 2018). This type of imaging technique uses a fluoroscope that continuously passes an x-ray beam through the body to gather real-time moving images of internal structures. The resulting image is transmitted to a monitor so the movement of a structure or contrast agent can be seen in detail (FDA, n.d.). During these procedures, the exposure to personnel is caused by scatter radiation from the patient. Typically, fluoroscopy systems are designed to reflect the photons that enter the patient toward the x-ray tube located below the patient surface (backscatter) in an attempt to direct all scattered radiation toward the floor. For minimal radiation doses, this setup significantly reduces the risks involved with radiation exposure. However, certain interventional procedures require substantial amounts of radiation doses so personnel must wear protective lead aprons to minimize exposure and risk (Dave, 2016). In EP procedures, fluoroscopy has often been used for guiding catheters through vessels and chambers of the heart in an attempt to reach the desired area for examination and

treatment (Cho, 2015). An example of catheter placement for an EP study to diagnose an unknown arrhythmia can be seen below in Figure 1.

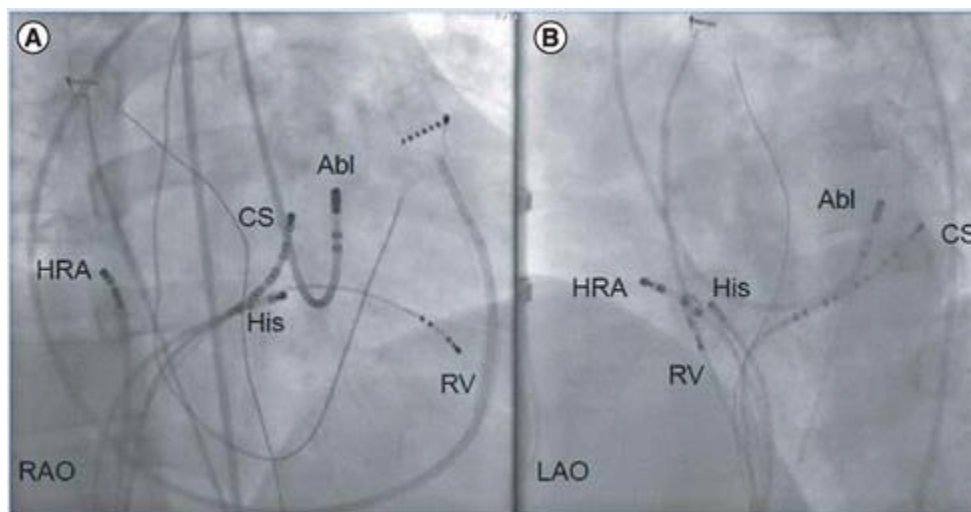


Figure 1: Typical placement of cardiac catheters during an electrophysiology study as seen through fluoroscopy

In general, when there is whole body exposure to radiation the threshold for acute hematopoietic syndrome (radiation sickness) is 500 mGy, acute gastrointestinal syndrome is 3000 mGy which is fatal without major medical intervention, and the lethal dose for 50% of the population in 30 days threshold is around 5000 mGy (Johnson, 1997). When adult patients are exposed to a 10 mSv dose, there is a 1 in 1000 risk that the patient will develop a solid tumor or leukemia and if the patient is exposed to fluoroscopy for more than an hour, the dosage absorbed can lead to skin damage (Wade, 1998). During radiofrequency catheter ablations, patients can have an average dose of 8.3 mSv for one hour of fluoroscopy (Vano, 1998). In recent years, the median effective dose over 3 years was 15.6 mSv with patients who repeat cardiac ablation procedures being exposed to more than 20-50 mSv (De Ponti, 2015). In regard to the cardiac catheterization lab staff, studies showed that these personnel are exposed to at least 6 mSv of

radiation per case with electrophysiologists averaging 4.3 mSv which equates to a fatal cancer risk of 1 in 384 but lead protective gear severely minimizes actual exposure amount (Venneri, 2009). Using 3D EAM systems to guide catheter ablation has proven to be a beneficial strategy for reducing radiation exposure. From 2015-2018, physicians analyzed ablation procedures at their institute performed under 3D EAM navigation between two groups with different frame rates of radiation. The first group had no restrictions on frame rate but had an average rate of 7.5 frames per second (fps) while the second group was limited to using only 3.75 fps. Procedural outcomes for these evaluations were successful ablations in 98% of the first group and 96 % in the second group. This indicated not only were there significant reductions in procedural time, fluoroscopy time, and effective dose, but using 3D EAM combined with a decreased radiation exposure time did not adversely affect clinical outcomes (Ali, 2021).

Catheters

Cardiac linear catheters are used in catheterization labs for ablation and diagnostic (recording and pacing) purposes during electrophysiology mapping studies (Joseph, 2012). They are typically made up of insulated wires that run through the catheter to connect to the distal tip electrode that is exposed to the intracardiac surface. Catheters usually come in different sizes ranging from 2 to 10 French, have electrodes that are typically 1 to 4 mm in length with an interelectrode distance ranging from 1 to 10mm. The catheters have the ability to obtain recordings derived from the electrodes that are either unipolar or bipolar. Unipolar electrograms (EGM) are typically used in applications where the physician is trying to determine the location of the catheter relative to the arrhythmic focus. As a signal propagates towards the electrode, the EGM displays a positive deflection. When the electrode is near or on the arrhythmic focus, the

signal will conduct away from the electrode resulting in an EGM that manifests a negative deflection. Bipolar EGMs are utilized when mapping regions of abnormal tissue that tend to produce high frequency, low amplitude EGMs. Unipolar mapping cannot detect these areas of scar due to the far-field signals from the higher amplitude healthy tissue nearby. Bipolar voltage recorded when mapping is a measurement of conduction time between two electrodes rather than measuring voltage of the underlying tissue. The interelectrode distance, electrode size and number of electrodes are important factors when attempting to record local voltage data, especially in areas of scar that contain low voltage (substrate). Catheters with smaller electrodes that are more closely-spaced are generally more insensitive to far-field components such as environmental noise and signals from larger regions with higher amplitudes that are typically detected with wider-spaced electrodes. The closer the electrode spacing, the more the fidelity of near-field signals is improved (Choudhuri, 2016).

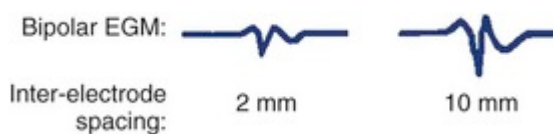


Figure 2: Example of a bipolar electrogram read by 2mm and 10mm spaced electrodes.

Figure 2 contains an example of how a more closely spaced bipole can accurately analyze and display the true local signal within the electrodes. Using the 10mm electrode spacing, the signal appears to have a larger amplitude which can be misinterpreted as a higher local voltage than actually exists. In this case, that signal is actually a combination of the local signal and far field signal acquired from another region of the heart with a high potential.

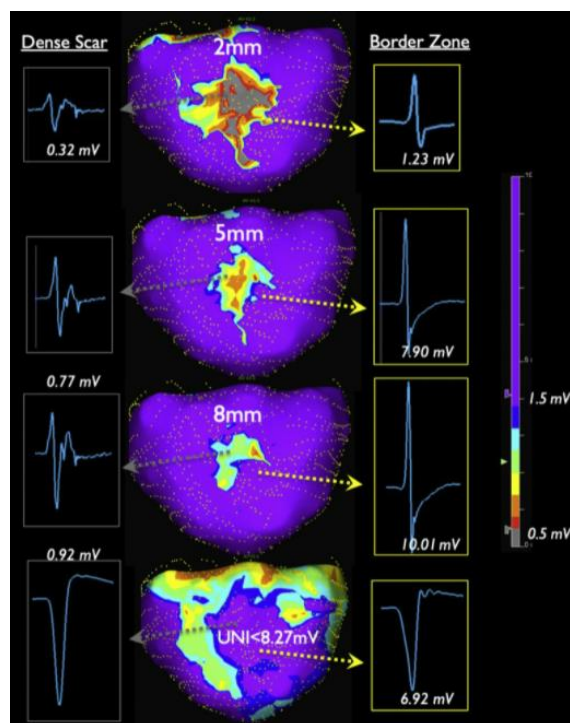


Figure 3: Voltage mapping of low-voltage substrate causing a reentrant tachycardia. Each voltage map represents differently spaced electrodes and how they interpret the local potential. It is evident that the 2mm spaced electrode acquires a more accurate representation of the low-voltage making it easier for the physician to determine an appropriate line of ablation.

The biggest concerns and limitations of linear and multi-electrode catheters in clinical settings are associated with bipolar blindness. During electroanatomic mapping, linear catheters only obtain bipolar recordings that document activation wavefronts that travel parallel to an electrode pair because the signal must be read by both the positive and negative electrode. When the wavefront travels perpendicular to the electrode spline, the catheter cannot read the signals so therefore the wavefront is ignored. This concept of bipolar blindness is crucial in cases where the patient has congenital heart disease that leads to low-voltage arrhythmia substrates and complex anatomies that linear catheters cannot record, possibly leading to failed ablation procedures

(Bryant. 2021). Companies such as Abbott, Biosense Webster, and Boston Scientific have designed multi-electrode basket, multi-spline and grid catheters that aim to overcome the issue of bipolar blindness. Multi-electrode catheters have the ability to acquire and interpret multiple voltage data points simultaneously in propagation directions that would be unseen by linear catheters therefore they acquire significantly more electrograms. However, Abbott's HD Grid is the only high density (HD) mapping catheter on the market to address bipolar blindness with every beat (Abbott, n.d.). HD refers to having a significant amount of data collected in the areas the mapping catheter is roving. High density mapping with HD Grid compared with Biosense Webster's Pentaray for cases where patients underwent VT ablation resulted in freedom from recurrent anti-tachycardia pacing at 1 year post-procedure in 97% and 64% of patients, respectively. This success is due to HD Grid's design and ability to utilize Abbott's best duplicate algorithm that allows for automatic comparison of bipolar and orthogonal electrograms to determine the better electrogram to be annotated for a given cathode (Abbott, n.d.). These results demonstrate that using HD Grid along with complementary mapping strategies improve long-term clinical outcomes in complex arrhythmia ablations (Proietti, 2021).

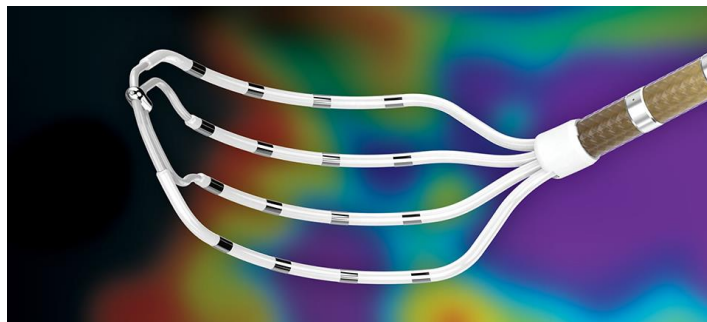


Figure 4: Abbott's Advisor HD Grid cardiac mapping catheter

Standard ablation catheters have several known limitations for substrate mapping and it's mainly due to the catheters being linear, average tip is 3.5mm, and interelectrode spacing

averages between 1-4mm. This results in center-to-center electrode spacing from the distal tip to the proximal electrode having an average distance of 3.25mm. At this separation, bipolar electrograms represent underlying tissue diameters ranging from 3.5 to 5.5mm (Leshem, 2017). Standard ablation catheters have the ability to differentiate between dense scar and healthy myocardium. However, due to the factors mentioned above as well as angle of incidence, vector of wave propagation, and filtering, they have insufficient sensitivity to characterize and accurately display myocardial bundles embedded in scar tissue. They can have difficulties interpreting these complex architectures of dense scar and geometry of cardiac anatomy. Multi-electrode catheters having smaller electrodes and interelectrode spacing increase mapping resolution because each data point recorded by the system represents electrical activity from a smaller tissue size (Tschabrunn, 2016).

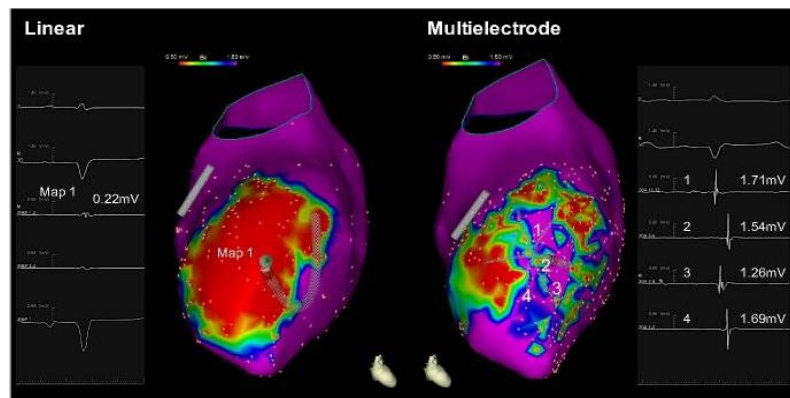


Figure 5: Voltage maps of the right ventricle using a standard linear catheter and a multielectrode catheter. The multi electrode catheter has the capability to map the low-voltage areas with more precision compared to the linear catheter.

When collecting data points to reconstruct the complex three-dimensional geometry of the heart using an EAM system, multielectrode catheters prove to be the better choice over standard ablation catheters. Ablation catheters containing a very minimal number of electrodes, often single-point sensors, are limited in terms of anatomical detail and accuracy that results in geometry with significant errors. Unlike standard ablation catheters, multi-electrode catheters are designed for acquisition of electrical and anatomical data from multiple electrodes simultaneously which allows for the rapid acquisition of chamber geometry. Early studies using linear multielectrode catheters combined with the Ensite NavX mapping system yielded models that were up to 94% accurate when dimensions measured were compared to MRI/CT scans of the modeled anatomy (Koruth, 2011). Like bipolar recordings for voltage mapping, collecting geometrical data from multi-electrode catheters has the best accuracy and yields the highest resolution when electrode spacing is 1-2mm and electrode size is less than 4mm (Bert, 2020). Abbott's LiveWire decapolar and duadecapolar catheters are widely popular around the United States due to their spacing as shown in Table 1 below. These catheters offer the appropriate number of electrodes for common procedures while containing the ability to accurately interpret local voltage due to their small spacing.

Regarding this project, the collection of geometric data points was recorded by Abbott's TactiCath, Sensor Enabled ablation catheter. As seen below in Table 1, this catheter contains 4 electrodes with a 2-2-2mm spacing and a contact force distal tip. This open-irrigated catheter consists of 6 irrigation holes with a 0.4mm diameter, a thermocouple for contact surface temperature measurement and a contact force (CF) sensor (Shenasa, 2019). CF sensing technology provides the clinicians and physician with real-time feedback on the catheter-tissue interaction during RF ablation through white light Fabry-Perot interferometer (Abbott, n.d.). This

interferometry allows the Precision system to make an interference analysis to compute the magnitude and orientation of the contact force for tactile feedback so physicians can adjust. Contact force combined with Abbott's algorithms for Lesion Size Index (LSI) and force-time integral (FTI) are found to reduce RF application time, reduce the quantity of ablation lesions, and shorten fluoroscopy and overall procedure times (Boles, 2017). Each physician has different target parameter values for these measurements during RF ablations to ensure effective lesions. By monitoring these values, physicians can also deliver safe lesions that minimize risk for complications such as acute vascular damage and steam pop (Alfonso-Almazan, 2019). Steam pops refer to the audible sound related to an intramyocardial explosion when the tissue being ablated using RF energy reaches 100 degrees Celsius. As mentioned above, mapping and collecting geometric data with ablation catheters will yield inaccurate and low-resolution models due to the larger size and spacing of the electrodes. Our system setup did not contain a CathLink Module pin block which hindered our ability to use diagnostic multi-electrode catheters for our testing and validation that would have resulted in more accurate geometries. The pin block allows users to plug in the pins that correspond with each electrode so that the catheter itself can be visualized and used on the mapping system. Without the pin block, users cannot connect any diagnostic catheters to the Precision software. The TactiCath ablation catheter contains specialized connections through the TactiSys Quartz and Precision Link equipment which allows the system to utilize this ablation catheter without the need of a pin block.



Figure 6: Abbott's TactiCath Sensor Enabled cardiac ablation catheter

Table 1: Popular Abbott ablation and diagnostic catheters			
Model	Electrodes	Tip Electrode Size (mm)	Spacing (center to center in mm)
TactiCath, SE (ablation)	4	3.5	2-2-2
FlexAbility (ablation)	4	4	1-4-1
HD Grid	16	(all electrodes 1mm)	3-3-3
LiveWire Decapolar	10	2	2-5-2
LiveWire DuaDecapolar	20	2	2-5-2

Cardiac Mapping Systems

Cardiac mapping is a term historically used to describe several conventions of recording and analyzing the electrical activity of the heart. These recordings may be a representation of the polarization cycles of the heart read by electrodes on the surface of the body by an electrocardiogram (EKG/ECG) or using an intracardiac electrogram (EGM) that displays local electrical signals recorded by electrodes from electrophysiological catheters that are strategically placed in anatomical locations within the heart. More commonly, cardiac mapping refers to an electrophysiology study that utilizes catheters that are introduced percutaneously into specific anatomical locations in the heart for the purpose of diagnosing complex arrhythmias by correlating local electrograms to cardiac anatomy. Newer cardiac mapping systems have revolutionized clinical electrophysiology by introducing three dimensional spatial localization through recorded mapping catheter locations and intracardiac electrograms that are used to create virtual three dimensional real-time model representations of the heart's chambers with color-coded electrophysiological information (Gupta, 2002).

In 2002, Anoop Kumar Gupta published an article that explored some of the best cardiac mapping systems at the time to explore their features and discover their limitations. The Endocardial Solutions (ESI) system was a non-contact intracardiac system that was designed to obtain cavity potential data from electrodes sitting in a pool of blood within one of the cardiac chambers and reconstruct them into myocardial potentials that are processed and displayed using a multi-channel amplifier and computer. The electrical array produced an image that allowed the clinicians to see the earliest activation of an impulse and a 'locator' signal from the catheter allowed them to move it towards that activation location. One of the main advantages of this non-contact system was that it only required one beat to reconstruct a complete activation map.

This allowed clinicians the ability to map hemodynamically unstable arrhythmias. Issues that arise from non-contact systems such as the ESI system were in regard to increased distance between the electrode array and the endocardium, specifically at distances greater than 34mm. This became clinically significant when inaccurate maps were created when mapping complex arrhythmias and anatomies such as dilated LVs or complex reentrant circuits (Gupta, 2002). Contact mapping systems such as the electroanatomic mapping CARTO system eliminated the inaccuracy due to distance by creating a system that utilized a mapping catheter's position and altitude in a low magnetic field produced from radiators positioned under the operating table. The main benefit of this system type was that it reduced the use of fluoroscopy, which exposed radiation to the patient and physician. This system determined the location and orientation of a reference and mapping/ablation 7-Fr catheter that were inserted into the coronary sinus and chamber of interest, respectively. The mapping catheter was dragged across the endocardium of the chamber and the electrogram from that contact allowed the system to generate a digital geometric figure. Systems similar to this CARTO system were of great value for guiding ablations because they provided information about the spatial location of the catheter in regard to the area of interest, but they were limited at the time because they were point-to-point mapping systems. PPM systems utilize single electrode catheters such as standard ablation catheters to gather data for maps one point at a time. However, this mapping technique was only suited for sustained arrhythmias or frequent recurrent premature contractions (Issa, 2009). These systems could only provide information about electrical potentials at the time of contact which means they could not account for non-sustained arrhythmias or physical movements and shifts.

These limitations were overcome by the more expensive systems at the time that processed and displayed information in real-time. One of the systems explored was the Cardiac

Pathways EP system that utilized two reference catheters and one mapping/ablation catheter to obtain information. The 6-F fixed curve distal shaft reference catheters were placed in the coronary sinus and the right ventricular apex and the 7F mapping/ablation catheter was free to move along the tissue of the chamber of interest. This system used an ultrasound transmitter that sent a continuous cycle of pulses to the three catheters that allowed the system to determine time delay between departure and reception of pulses, thus calculating distances between catheters and creating a 3D reference frame. Since the pulses were continuous, the computer was able to continuously triangulate the position of catheters and update the object within the 3D reference space. This style of mapping was a major development in the EP field but still had limitations such as the failure of ultrasound transducers and the inability to produce a voltage map using only ultrasound technology. The systems made a significant impact for physicians guiding catheters during ablation procedures to treat unstable arrhythmias, but they could not fully rely on these systems to produce all of the images they needed because each system had its limitations on what maps and data it could display. Systems that were developed after these needed to incorporate all of the critical features of each of these systems while still keeping patient safety in mind.

Both contact and non-invasive mapping systems developed rapidly by the time contemporary mapping techniques for identifying and modifying arrhythmogenic substrates were studied in the mid 2010's (Koutalas, 2015). The contact systems used for these studies were Biosense Webster's CARTO and St. Jude's EnSite NavX Velocity electroanatomic mapping systems. Through the combination of active weak magnetic fields, magnetic catheter tips, and electrode patches located on the patient's body, the CARTO system allows the clinician to produce a 3D matrix map that continuously measures the strength of the magnetic field and

calculates the catheter's exact location (Romero, 2016). The EnSite NavX Velocity system used six skin electrodes to create a 3D coordinate system using high-frequency electric fields.

Impedance based gradient-calculation systems like this localize catheters relative to their position from a reference pad and overcome the body's non-linear impedance to create a three-dimensional map that was more accurately representative of electrical activity and geometry of the chambers. Clinical research performed with contact-based systems demonstrated that implementing contact force, image integration, and hybridization are technologies necessary for progressing toward more effective mapping and ablation of complex arrhythmias. This research also showed that visualizations of low-voltage/scar surrogating fibrosis allow physicians to effectively eliminate arrhythmogenic substrates to change the prognosis of patients suffering from highly symptomatic ventricular and supraventricular arrhythmias. Areas of fibrotic substrate are difficult to image so physicians rely on low-voltage maps to inform them on the paths of electrical conduction between the substrate that are causing these arrhythmias. These systems show the significance of having real-time feedback on multi-electrode high-resolution mapping based on catheter-tissue interaction, but limitations still needed to be overcome to improve success and accuracy rates. Magnetic based systems use a location reference attached to the patient's back so any movement of the heart relative to the patch will cause the map to shift and become inaccurate and sometimes unusable. These magnetic systems have the ability to account for any movement of the patient during the procedure because the surface reference will move with the patient. With impedance based systems, system references are intracardiac electrodes, such as the electrodes of the CS catheters, so a physical movement of the heart will not affect the maps. However, using an intracardiac reference causes impedance based systems to be insensitive to potential patient movements. The hybridization of magnetic and impedance

field data developed by Abbott with their EnSite Precision cardiac mapping system alleviated the limitations that previous systems experienced individually (Koutalas, 2015).

EnSite Precision

The system we used to integrate with our wet lab was Abbott's EnSite Precision cardiac mapping system. The Precision system provides highly detailed anatomical models and maps using a hybrid of impedance and magnetic field data to effectively diagnose and treat a large range of arrhythmias. To collect impedance data, 3 pairs of surface electrodes are placed along the 3 orthogonal axes (X-Y-Z) and a reference patch is placed on the patient's abdomen to form a three-dimensional electrical field on the patient's thorax. The first pair of patches are placed on the patient's mid-chest and back, the next pair is placed on the right and left side of the thorax, and the final pair is placed on the back of the neck and left inner thigh which creates the Y, X, and Z axes, respectively. To create an impedance field, an 8 kHz signal is emitted alternately through each pair of surface electrodes which creates a voltage gradient along each axis (Abbott, n.d.). Conventional or Sensor Enabled EP catheters are connected to the Precision system and advanced into the transthoracic electrical field where they acquire the voltage emitted from the surface electrodes. These voltages, timed to the creation of the gradient along each of the axes, are processed by the Precision system and the three-dimensional position of all catheter electrodes are calculated simultaneously. This calculation allows for real-time visual navigation of all catheter electrodes that are within the transthoracic field. The catheter electrodes are displayed according to their respective catheter (ablation or diagnostic) and real-time motion of these catheters enables the system to create three-dimensional electroanatomic models of the cardiac anatomy.

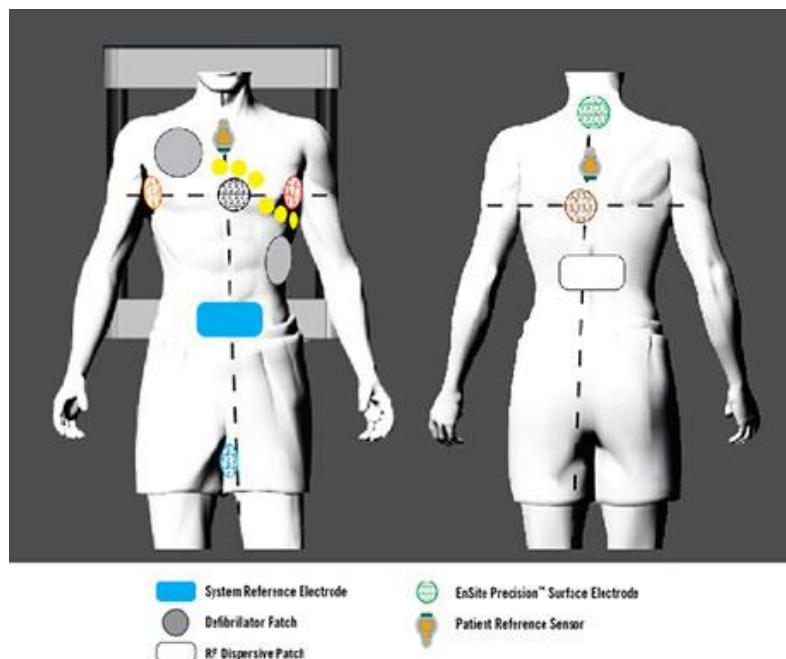


Figure 7: Placement guide of surface electrode patches, system reference patch, patient reference sensors, defibrillator patch, and RF generator patch relative to the Precision Field Frame

The addition of magnetic data has not only allowed the Precision system to be competitive with other magnetic-based mapping systems on the market, but it has also significantly improved the quality of maps generated by the system. The EnSite Precision Field Frame mounted underneath the patient bed generates a low-powered magnetic field that Sensor Enabled devices and tools can be detected in through a connection to the Ensite Precision Link, Sensor Enabled. Two patient reference sensors (PRS anterior and posterior) are placed near the front and back surface electrodes and function as sensors for patient movement and metal distortion. Using these sensors in conjunction with Sensor Enabled catheters, the NavX Navigation software utilizes its Sensor Enabled Field Scaling module to dynamically optimize the model and map. It does so by adjusting dimensions of the data points within the navigation field using known offsets between the position and orientation of the PRSs and surface

electrodes. The same is true for monitoring field stability for unexpected patient movements such as coughing or snoring. The EnSite Precision system has highly improved accuracy, resolution, and stability compared to its predecessors, the Ensite NavX and EnSite Velocity. This is due to the Precision's ability to increase accuracy of less than 1mm with the addition of magnetic field-based localization data that refines the impedance-based tracking in real-time (Shenasa, 2019). In various cases involving electrophysiology mapping and RF ablation, the EnSite Precision mapping system was associated with trends of low mapping times, high system stability, and high rates of acute procedural success (Issa, 2009).



Figure 8: Sensor Enabled PrecisionLink (left) and Precision Field Frame (right)

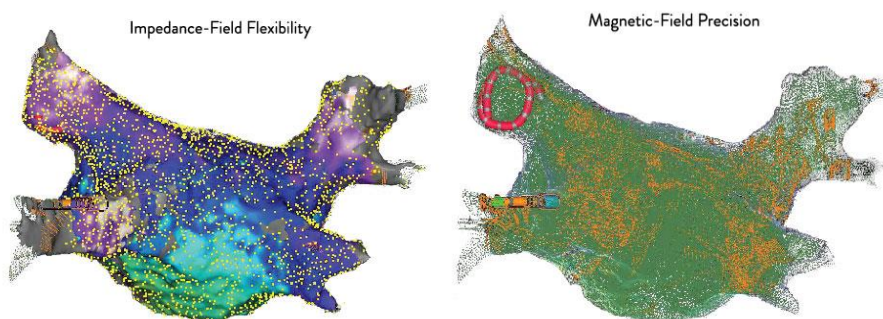


Figure 9: Voltage maps of the left atrium and pulmonary veins before RF ablation to isolate the pulmonary veins to treat atrial fibrillation. The image on the left represents impedance-field data points and the map on the right displays magnetic-field data points.

InVitro System

A key component to successfully integrating the Ensite Precision to Cal Poly's wet lab included designing an in-vitro tank. The main goal of our project, however, was to specifically design an in-vitro chamber that is compatible with Abbott's (Ensite Precision) and allow cardiac mapping to be performed. Our end goal was to create a system where faculty, students, or companies can validate their projects, designs, and products. Another benefit of the in-vitro chamber is for educational purposes. With further development of the in-vitro chamber, physicians and faculty members will be able to perform experiments to demonstrate differences in lesion, formation dependent on tip-electrodes, sensor technology and ablation techniques, influence of blood flow and electrode-angle to the myocardium. Our aim for this project is to promote a Learn-By-Doing environment through our wet lab design.

Before designing our chamber, research was conducted on existing wet labs and in-vitro chambers. The main goal of assessing these systems was to learn what instruments were required in a successful system. By researching the required instruments, we planned to order the equipment early in the quarter and make note of what to include in our design. Another reason for reviewing studies was to find more information on the specific design of in-vitro tanks that these studies were performed in.

In a study done by Calzolari, an in vitro model was created to test two hypotheses: 1) lesion dimensions correlate with lesion size index and 2) LSI could predict lesion dimensions better than power, contact force, and force-time integral (Calzolari, 2017). The purpose of the study was to determine a reliable predictor of lesion quality when radiofrequency catheter ablation for cardiac arrhythmias were performed. Calzolari and his team created an in-vitro

chamber to test the validity of LSI, a multiparametric index incorporating time, power, contact force (CF), and impedance recorded during ablation shown in Figure 10.

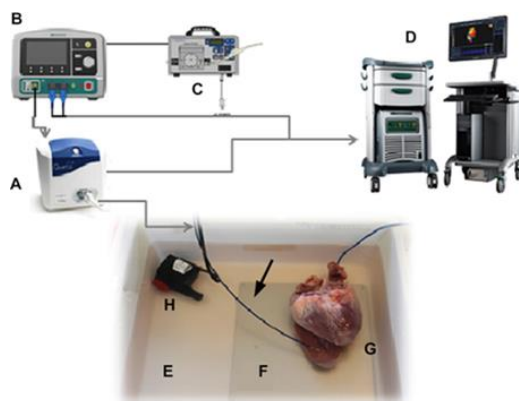


Figure 10. Cazolari's In-Vitro Experimental Set-up: A) Contact force catheter interface, B) Ampere RF generator (St. Jude Medical, St. Paul, Minnesota) C) Coolpoint irrigation pump (St. Jude Medical), D) NavX electroanatomic mapping system (Endocardial Solutions, St. Jude Medical). (E) Saline bath. (F) Ground platform. (G) Porcine heart. (H) Non-pulsatile pump. (Arrow) TactiCath ablation catheter (St. Jude Medical).

In Figure 10, the arrow is a TactiCath Quartz catheter that was mounted in a fixed standard 8-F, 11-cm sheath that manually maneuvered over a ground platform placed within a tank filled with circulating physiological saline solution at room temperature. Within the circulating bath, a pump is used to produce a non-pulsatile flow directed perpendicularly to the myocardium surface at a rate of 5 L/min. The animal tissue used in the experiment were fresh porcine heart muscle slabs (mid-myocardial layer of the left ventricle) with a thickness of 2 to 4 cm. The Coolpoint roller pump by St. Jude was connected to the catheter and delivered a saline solution at 17ml/min during the RF delivery. The Ampere RF generator also from St. Jude Medical was connected to deliver 550 kHz unmodulated sine-wave RF energy pulses in a

temperature-controlled mode (Max 41°C). Lastly, contact force, temperature, impedance, FTI, and LSI values were monitored during RF delivery via Ensite mapping system. Cazolari's study was beneficial to the design requirements of the project because Cazolari's study involved some of St. Jude's equipment that were also available in the lab for us to use. For ablation the flow rate, RF energy pulse temperature range and the unmodulated sine-wave frequency used in Cazolari's study would be emulated.

In another study performed by Deno, a controlled wet lab bench testing was designed to quantitatively explore correlations of electrical coupling index to applied force between the catheter and tissue, depth of penetration, and angle of contact between the catheter and tissue. Although the goal of the study does not align with the scope of our project, the study provided details on its bench testing set up. For this study, a ventricular tissue was sectioned in 1.5-2cm slabs to create a uniform tissue surface and was placed in a Pyrex chamber filled with a 20 C mixture of saline and water to a blood-like conductivity of 6.2–6.8 mS/cm (Deno, 2014).

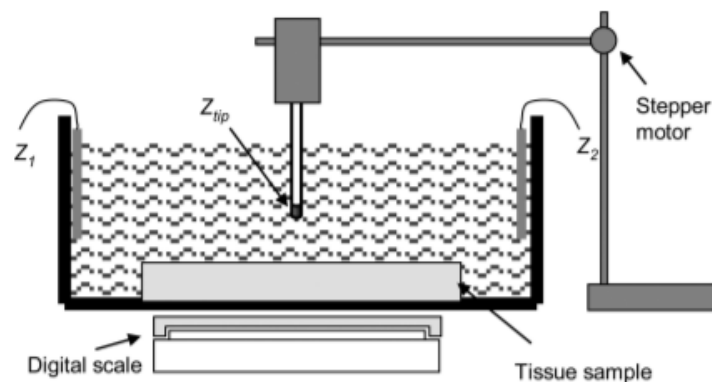


Figure 11. Setup for bench model experiments: Freshly excised beef heart tissue was submerged in 20 C saline. Force, vertical displacement, as well as complex impedance and ECI were measured as an ablation catheter tip approached and entered into heart tissue. The 90 ° angle of contact is shown (Deno, 2017).

Saline Solution

After review of Cazolari's and Deno's lab apparatuses, more questions regarding how saline solution affects ablation arose. More research was performed to help understand why Cazolari and Deno might have chosen the values they had for their saline solution. For regular ECG patches, a patient is advised to wipe off any dead cells on the skin with an alcohol wipe. Afterwards, a conductivity gel is applied to the patch to pick up the extremely tiny electrical impulses of the heart. Similarly, because Abbott's patches do not come with conductive gels, we must create an environment for electrical impulses to pass through the medium. By adding salt to our solution, the impedance is lowered, which allows clearer signals to pass through and be read by Ensite Precision.

Results from a first in-human early feasibility study using a saline enhanced radiofrequency thermal-ablation system to treat ventricular tachycardia suggests a highly feasible approach to treating patients with recurrent ventricular tachycardia that is resistant to "other treatments" (Packer, 2020). More common treatments include implantable cardioverter defibrillators, medical therapy, and other forms of ablation therapy. This study was innovative for its time in that it was first to use a needle electrode to deliver heated, degassed saline and radiofrequency energy into the tissue. A five-month follow-up data of the 32 patients from the study showed that more than half of the patients had no recurrent ventricular tachycardia, and more than 60 percent of the patients had their disease reduced by 90 percent or more. Packer demonstrates the benefit of saline RF ablation through this study, and the importance of this practice is noted for when ablation will be performed in our tank.

Another interesting study regarding saline ratio was done by Hong and Glover. The standard irrigated radiofrequency ablation is performed using normal saline 0.9%. However, the

study compares the effectiveness of ablation using half normal saline 0.45% to normal saline (Hong, 2019). Hong and Glover demonstrated that by decreasing ionic concentration in radiofrequency ablation, the frequency of recurrences of conduction was increased. The study does not directly relate to our tank as we do not plan to prioritize ablation but provides information that saline concentration does affect the effectiveness of ablation. In a different study performed by Pierre Jais, Biosense Webster's catheter was used using a 0.9% saline and recorded successful data. Based on existing literature, we have decided that 0.9% saline is generally accepted for ablation procedures, but we would have to look at how different saline concentrations would affect our images.

Cal Poly's Wet Lab

Cazolari's and Deno's models were the two wet lab systems we decided to adapt to our design. We decided to adapt their set-up to our model because our goal was to create a tank for mapping and hopefully be able to perform ablation procedures afterwards. Both studies documented key equipment necessary for RF ablation in our tank, material choice of the tank, importance of saline solution, and tissue specimen and size for ablation.

The purpose of Cal Poly's wet lab is to develop a functioning wet lab that will be integrated with Abbott's EnSite Precision Mapping System. The system will then allow for industry to partner with Cal Poly to perform testing of products like catheters, sheaths, and etc. The tank will also open new avenues for student projects in clubs such as EMPOWER and Medical Design Club. Students will be able to utilize the lab to work on projects related to catheters, electrical mapping, and ablation. Another tool the wet lab can provide for Cal Poly is an environment to perform educational student labs. Dr. Porterfield or other faculty members are

able to demonstrate ablation procedures or instruments used in the surgery room in a more hands-on environment. Faculty members from both BMED and other departments are also able to incorporate the lab into their curriculum.

There are steps that had to be accomplished for a successful wet lab. First, with the help of Sarah Griess, Abbott's equipment and software was set up in Cal Poly's ATL. In a span of two to three weeks, Sarah was able to install the software to the PC in the lab and made sure all the equipment worked properly. After all the equipment was set up and running, we moved on to designing our tank. We spent time researching After the tank was manufactured, a leak test and pressure test was performed to test the integrity of the tank. Once the tank was validated, integration of Abbott's system to the tank followed. After successful integration, validation testing of the system was performed.

Specification Development

. The start of the project consisted of a few weeks of brainstorming ideas with the sponsor to define the scope and direction of the project. We proposed that we sought to be part of an applicable project in the field of electrophysiology. The sponsor, Dr. Porterfield, suggested a project involving the Ensite Precision Cardiac Mapping system donated by Abbott. This system is located in the ATL (Advanced Technologies Lab) at California Polytechnic University's campus. After our discussions, we concluded to design a system for Dr. Porterfield to be able to demonstrate procedures he would perform in hospitals in a classroom setting for his students.

The general goal of the project was to create a wet-lab that includes an in-vitro chamber to perform tests by integrating the Abbott device and produce images of whatever we are trying to map within our chamber.

The scope of the project was defined in further detail as installment of the system in the ATL and testing its functionality. Once the system is functional, the next step is to build a tank that simulates an "in-vivo" environment that can be integrated with Abbott's Ensite Precision Cardiac Mapping System. Once successfully integrated, the next goal is to obtain images in the tank using the system.

This environment can serve as a space on campus that can be used for various situations. For one, Dr. Porterfield would use this space as intended to demonstrate procedures in detail for his class. This is beneficial in that Dr. Porterfield, or any other individual can offer a more detailed explanation of his procedure on a sample. This procedure can also be demonstrated to a larger number of students than his usual "shadowing experiences" offered at the French Hospital. Another benefit of this newly developed lab would be allowing future faculty or student projects involving medical devices such as catheter, stents, heart models, etc. to be tested

in our designed system. Once deemed accurate and precise, Cal Poly's new cath lab can be used by medical device companies to test their products.

After a few weeks of defining the project and agreeing on a feasible scope of the project, our next goal was to create project success criteria: more detail of what is required for this project to be successful is shown in Figure 12.

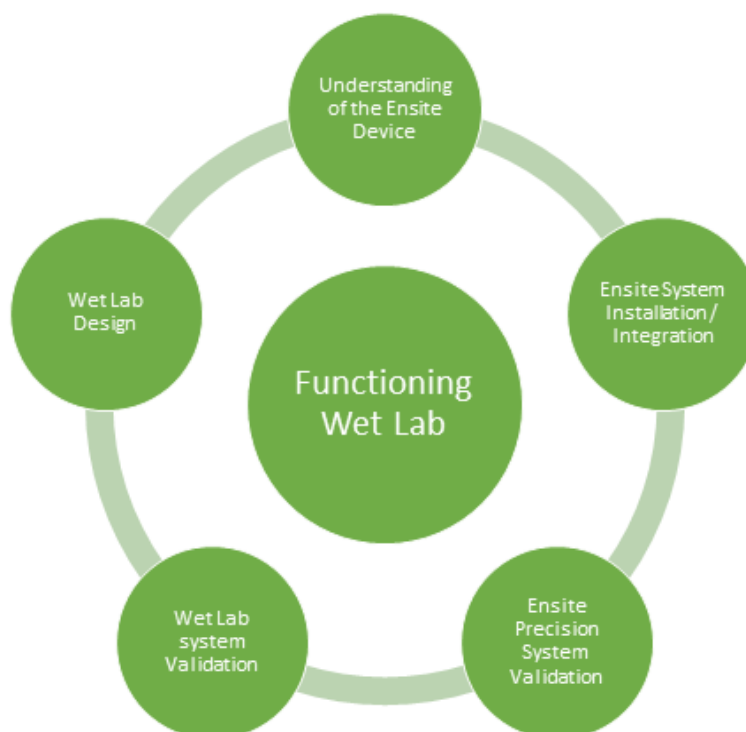


Figure 12. Required Components of a Successful System: Diagram to show components that make up a successful functioning wet lab for this project.

For the project to be successful, we must first have a basic understanding of the system. We are responsible for understanding the functions and capabilities of the device. We must also be aware of the safety and risk hazard the device imposes. By gathering basic information of the system before the integration, we hope that the gathered information will make the process of setting up the device and the integration smoother in the future. During the project, we are not

responsible for improvement on the software & hardware of the system provided by Abbott nor the maintenance of the device. The device will be initially installed by an Abbott Representative.

A crucial part for the overall scope of the project is the wet lab design and the integration of the tank to the existing system. Our team must be able to prototype and manufacture a device that can be successfully integrated with Abbott's Ensite Precision Mapping system. The device must be able to hold a large volume of saline solution, maintain temperature, and station six leads from Abbott, as well as allow a mapping catheter to be smoothly maneuvered. Once such a tank is designed, validation tests will be performed to measure the functionality of the tank. After validation of the tank and a successful integration, we plan to create a study to test for accuracy of the device and the system involving images generated from our tank. The study is designed to demonstrate accurate integration of the system. The manufacturing, integration, and testing processes of our project should also provide insight and limitations of wet lab testing.

Once the project success criteria were defined, the next step was to define our design specifications. We listed factors that would limit our design and made a list of parts of the project that were key factors.

Specifications we focused on early were:

1. Dimensions of the chamber
2. Material of the chamber
3. Saline solution (concentration/volume)

For dimensions of the chamber, several factors were considered. The max dimension for the tank is limited by the size of the table in the ATL (64 by 37.2 inches.). The tank must have a space that allows a sample to be placed. Another dimension limitation was the dimension of the magnet of the Ensite Precision system. The sample we plan to map needed to be placed within

the magnet with the dimension of 11 by 11 inches. Therefore, we determined a cube with a side length of 6 to 8.5 inches would be a reasonable dimension for the samples we would be mapping. The length of the tank was determined by researching the average length of a human adult (18 to 20.5 inches). Maximizing the space for our sample to 8.5 inches, would result in the remaining length of the tank to be 11.5 inches. It is important to note that increasing the dimension increases the amount of saline solution placed in the tank. Greater amount of saline solution increases the pressure the walls experience.

Regarding the material of the tank, the literature review showed that all of the table-top ablation models were built using acrylic. Acrylic is an acceptable material of choice due to several properties. Being clear, acrylic allows the model to be observed while being mapped. Acrylic is also a great material for manufacturing for us with the given tools and machines in Cal Poly's machine shops. We used Matweb's database to obtain more information on mechanical properties of commonly used acrylic shown in Appendix B.

We looked at the hydrostatic forces the walls of the tank would experience once the tank was filled. In larger tanks, the pressure is greatly affected by the depth. The calculation of the max stress our tank would experience can be found in appendix A. The density of our medium (normal saline) is $1,045 \text{ kg/m}^3$ compared to that of water (1000 kg/m^3). The maximum hydrostatic force exerted was calculated to be 25.7 N. Using this force with the smallest area of the wall of the cube, the stress was calculated to be 20.44 Pa. It is important to note that our stress experienced is significantly smaller than the stress allowable by the three material choices from MatWeb, so we determined using any of these materials would not cause fracture and bending of the tank. We decided to use Optix Acrylic sheets as it met the required mechanical properties and was less expensive than other material choices,

Through literature review and discussion with Abbott Engineers we decided to use normal saline (0.9%). Instructions for making normal saline can be found in the appendix G in “saline manufacturing process.” The reason we decided to use normal saline was that modifying the concentration has an impact on ablation but a miniscule impact on mapping. Also, normal saline is the generally accepted solution used in many of the studies, so we believed it was best to emulate the standard solution. Keeping the specifications we defined above in mind, we moved on to concept generation.

Concept Generation and Evaluation

Throughout the year, the project's concept generation followed the diagram shown in Figure 13. Once the specifications were defined, we created our first prototype (initial version) during fall quarter. During winter quarter, after performing validation testing on the tank and seeing flaws of our prototype, further development was made, and several intermediate versions were created. Input from engineers at Abbott, failures during testing, modifications for ease of use, and change in manufacturing process were all part of the development phase. As we discovered that our winter quarter's final prototype was functional, we decided to create a final version of the prototype by making small modifications such as dimension changes. This section will outline the details of the various versions we went through and our reasoning for the small adjustments made throughout the year.

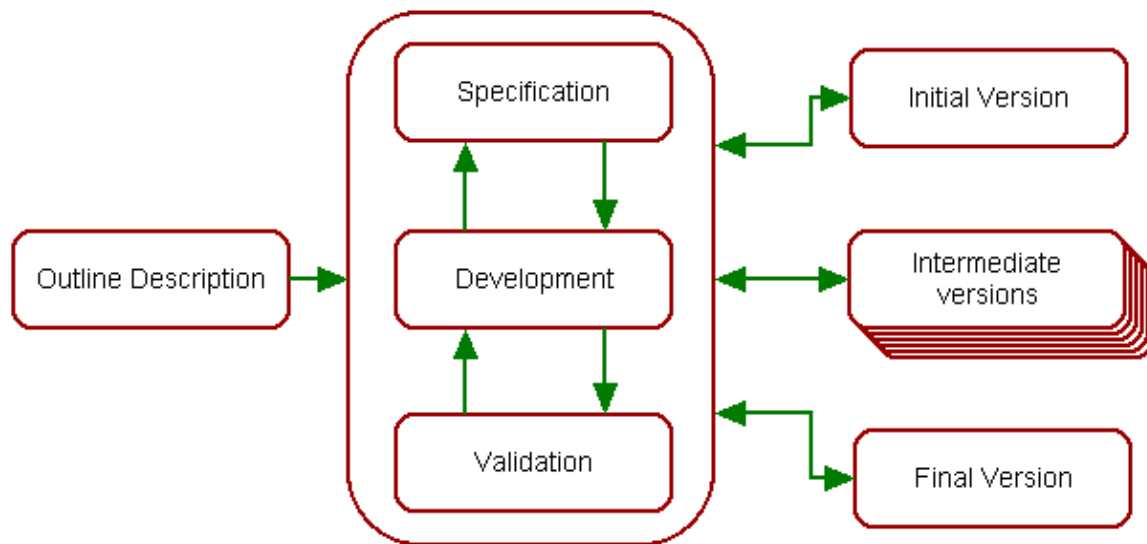


Figure 13. Flowchart of Concept Iteration: The diagram outlines our methods of concept generation and design of various versions while performing validation testing. [14]

The original concept was generated through literature review. After reviewing three studies of existing in-vitro chambers used for training biomedical engineers or for RF ablation procedures, the designs of the chambers used in these studies were adapted in our concept generation. From these studies we came up with the idea to add a non-pulsatile pump, a CoolPoint roller irrigation pump by St. Jude, and a ground platform within our chamber.

After talking to Sarah Griess, we realized that we needed to accommodate our tank for the magnet dimensions in our dimension for the chamber and were provided equipment from Abbott that we could use in our project. From this information, the dimensions of our chamber were slightly adjusted. The magnet required the tank to be 3 in. above the surface of the table, and a wooden fixture was built for the tank to sit on during testing. Another change that was made was the overall dimension of the tank. We initially thought that we needed a hexagonal shape for the placement of the patches and built the tank to have a length of 18.5 inches (the average length of an adult torso). After a series of validation testing on the tank, we learned that the tank can still be functional with a cube instead of a hexagonal prism. Also, the tank's overall width, length, and height was reduced to decrease the volume of saline solution needed for the experiment. Once the tank was able to endure the volume of water placed in it for the required time, we moved on to the integration of the tank with Abbott's system.

During the integration, there were several issues that arose. A problem we faced was the Ensite Precision system not being able to identify our patch placements. Despite our expectation of being able to read electric signals through the acrylic panes, there were no signals being picked up. After several troubleshooting efforts, we decided to make square cuts on each pane and aluminum cut outs for the electrode patches to be placed; the patches were functional after

this adjustment. Once this final adjustment was made, our prototype was deemed functional with Abbott's Ensite Precision Mapping System.

For the final concept, the dimension was slightly adjusted: the height of length of the tank was brought down to touch the floor to reduce stress failure at the joint and also to lower the location of the electrode placement of the leg electrode. Another final adjustment to the tank was to make a "holder" on the insides of the tank for a lid to sit into the tank for the chest electrode to be in contact with the saline solution.

To summarize our concept generation and evaluation, it began with outlining the goal of the project, defining specifications, and rapid prototyping to generate a model. Once the model was created, validation testing on the model and integration of the model to the system led to modifications on the existing design. The culmination of the minor changes on different versions have led to our final prototype, which is not only functional, but also with a more defined manufacturing process and easier to use during testing than the previous versions.

Conceptual Models and Analyses

Throughout the year, our conceptual models changed through literature review, discussion with our sponsor and Abbott engineers, through manufacturing processes, and through test and validation. The three main concepts were: a box, a hexagon, an octagon. This section outlines our process leading up to different concepts as well as the analysis of the benefits each concept brings.

The Box Model

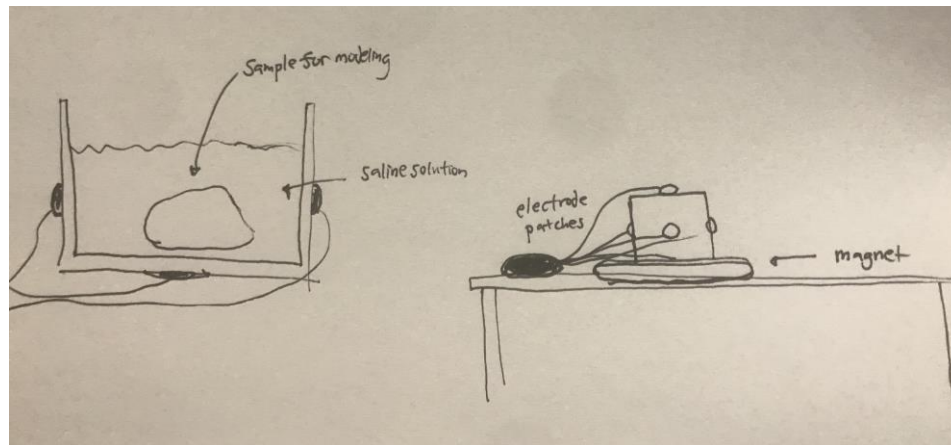


Figure 14: Concept Sketch of Box Model

The box model was adapted from existing studies. The design consisted of a rectangular box that would contain saline solution and the tissue of interest while we used Abbott's Instruments to create images. The box concept was considered because literature review demonstrated that this design was functional and seemingly easy to manufacture. The benefit of following through with this concept would be that we would be able to manufacture multiple prototypes easily and begin testing and collecting data as soon as possible.

Hexagon Model

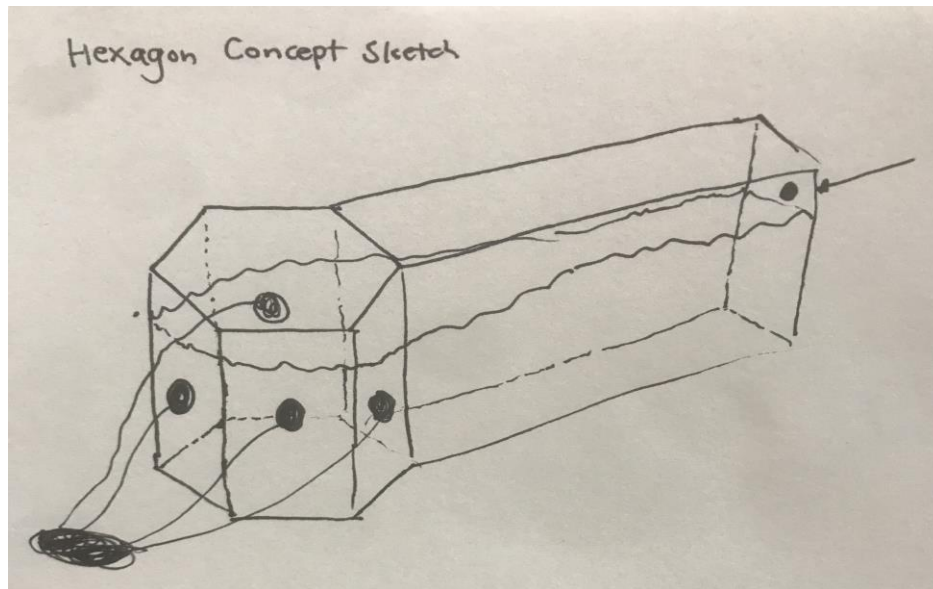


Figure 15. Sketch of Hexagon Model Concept

As previously mentioned, Abbott's system requires six total patches to be placed on the tank. Instead of having one patch placed on each face of a cube as in the box model, the hexagonal model allows five patches to be placed on the rectangular faces of the hexagonal prism and the reference patch on the base. A rectangular prism was added to serve as a pathway for the catheter to travel to the target sample. This concept is beneficial in that it fulfills the goal of education use. The rectangular part of the tank serves as a way for Dr. Porterfield to demonstrate procedures to students by guiding a catheter through the "torso" of the tank to the sample meant for mapping.

Octagon Model (Prototype I)

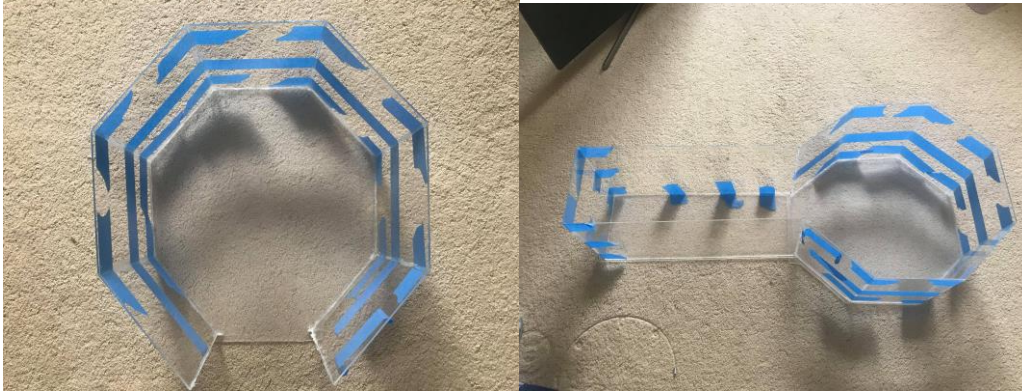


Figure 16. Octagon Model: Physical model of octagon model drying after fabrication.

After performing validation testing such as leak and pressure test and learning more about the integration process, we realized that our tank needed design modifications. We learned that the hexagonal model setup was not functional for the integration of Abbott's system. The six patches needed to be in specific locations in relation to one another. The Octagonal model was proposed so that the chest patch is placed on the lid, the left and right-side patches placed on the parallel side panes, the neck patch is placed on the base of the octagonal prism, the leg patch is attached to end pane of the rectangular prism, and the reference patch placed on the base of the rectangular prism. After setting up the patches like so, we were able to get readings on the system that the patches were attached to. Because the system is designed to be placed on patients of different body sizes, the location of the patches, more so than the distances between the patches, was important. Another error we found during integration testing was patch signal errors. To increase the sensitivity of the signals, square cuts were made on the acrylic where the patches would be placed. On those square cuts, an aluminum sheet metal was cut to size and sealed with a marine sealant.

Prototype II

To address the issues with Prototype I, Prototype II was scaled down to a rectangular prism with a dimension of 6in. x 8.5 in. x 8.5 in. and a rectangular prism 4 in. x 10 in. x 6in. attached to the end. The patches were placed in a XYZ orientation as rectangular prisms were sufficient for patch locations. The dimension of the tank was reduced to decrease the hydrostatic force exerted by the volume of saline solution. While designing the new tank, we also decided to buy a thicker pane for our acrylic. The increased thickness provided more stability where the panes connected as well as endured more pressure applied vertically and horizontally.

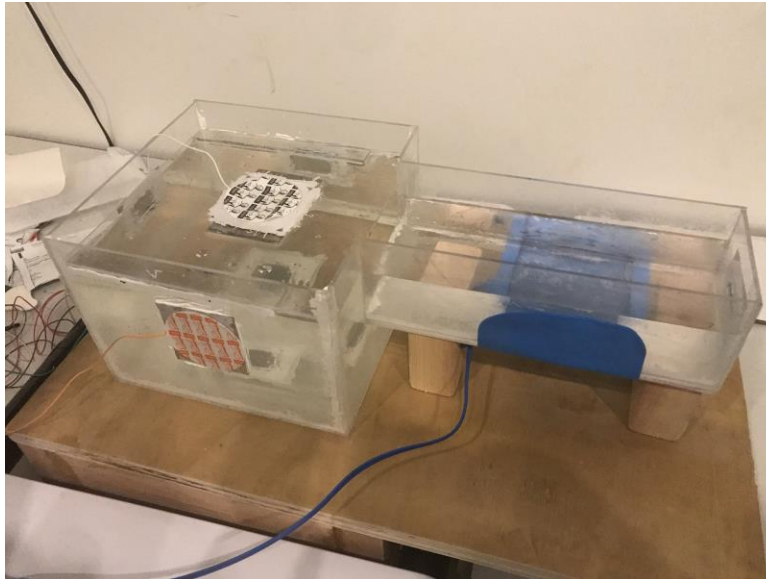


Figure 17: Prototype II model set for integration testing of the system

Final Prototype

The final prototype was created towards the end of the spring quarter as integration testing was performed. The changes made to the final prototype were minor dimension adjustments to the tank and a dimensioned design for the lid for the chest electrode to be placed. The rectangular cut was enlarged to increase surface contact with the reference electrode. The

rectangular prism that was once elevated was brought down to be in contact with the wooden platform to reduce stress where the cube and the rectangular prism are joined. The dimensions and drawings for the model can be found in appendix C.



Figure 18. Final Model Prototype: A) Final Prototype; B) Final Prototype under testing

Prototype Manufacturing

The manufacturing processes for our prototypes were adjusted as different versions were created. Ultimately, the process began with cutting the acrylic into pieces that build into the tank, apply epoxy and sealant to glue the pieces together, and let the tank rest and dry.

At first, most of our prototypes were manufactured through machining. The acrylic was measured out by a yardstick and machined using a table saw, a miter saw, and a band saw. The tools that we used were from both Mustang 60 and The Hangar on Cal Poly's campus. The detailed manufacturing instructions for cutting acrylic and gluing acrylic can be found in the appendix F.

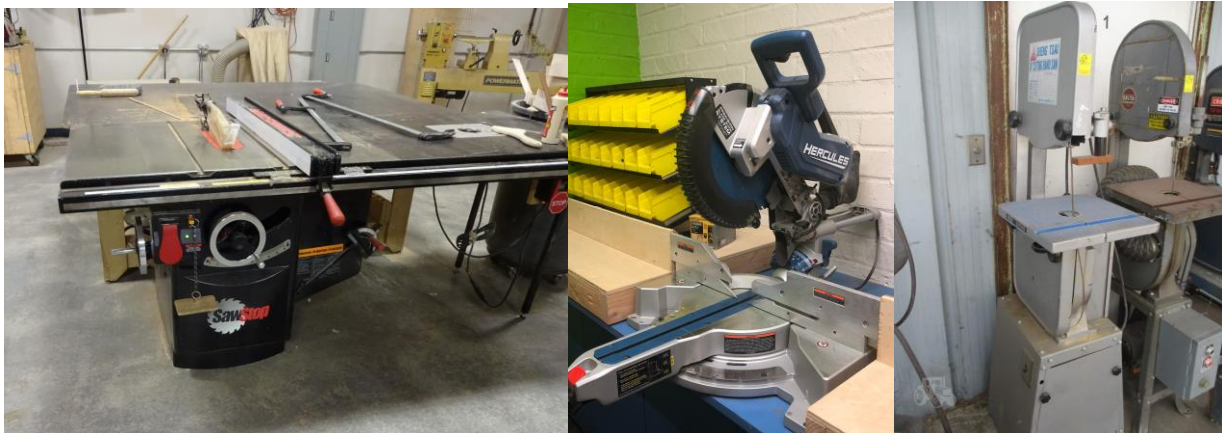


Figure 19. Tools Used for Manufacturing: A) Table Saw; B) Miter Saw; C) Band Saw

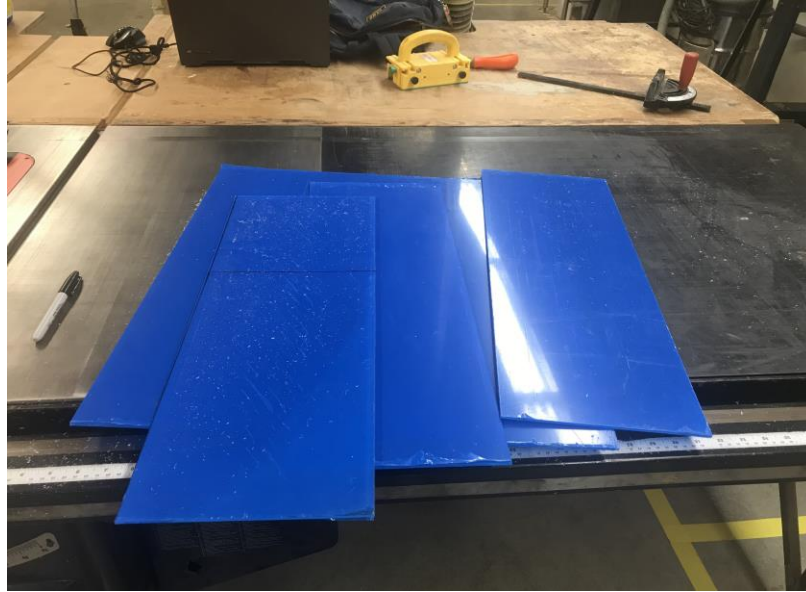


Figure 20. Pieces of Acrylic cut in Mustang 60

For our final prototype, we decided to laser cut the acrylic in Mustang 60. The benefits of laser cutting were improvement in accuracy of the cuts and decrease in manufacturing time. The disadvantage of laser cutting is that compared to the machines, laser printing in the shop requires appointments and setting up the drawing files for laser printing. However, once all the drawing files were prepared, the time for cutting was reduced from two to three hours of machining to thirty minutes of laser cutting. As previously mentioned before laser cutting, one must have SolidWorks parts for the dimensions that need to be laser cut. Once all the parts are designed, each part is saved as a drawing (dwg) file. The software that is used in Mustang 60 to interact with the laser-cutting printer is Adobe Illustrator. After the dwg file is opened in a template in Illustrator, it is positioned on the screen as it is desired to be cut. The specific instructions of using the software and the printer to laser-cut acrylic will be included in appendix F.

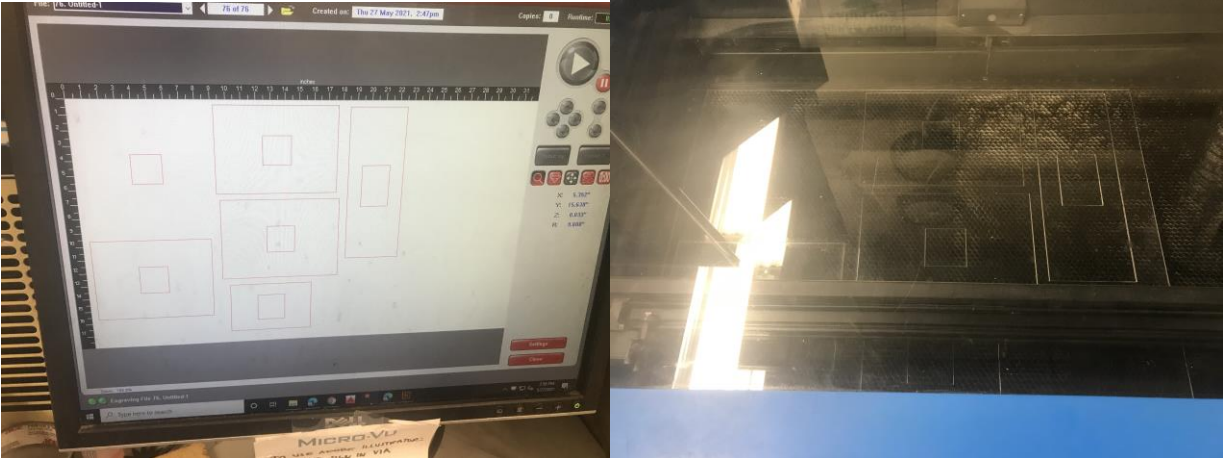


Figure 21. Process of Laser Cutting Acrylic: A) Laser cutting software that outlines cuts that will be made on the acrylic piece. B) Physical cuts on the acrylic sheet made in the printer.

For the aluminum sheets, we used the foot sheet metal shear in the Aerospace Hangar to make cuts. After measuring out the dimensions on the aluminum sheet, we insert the sheets into the machine. Once inserted, a person can step on the lever, to make a shear cut on the sheet.

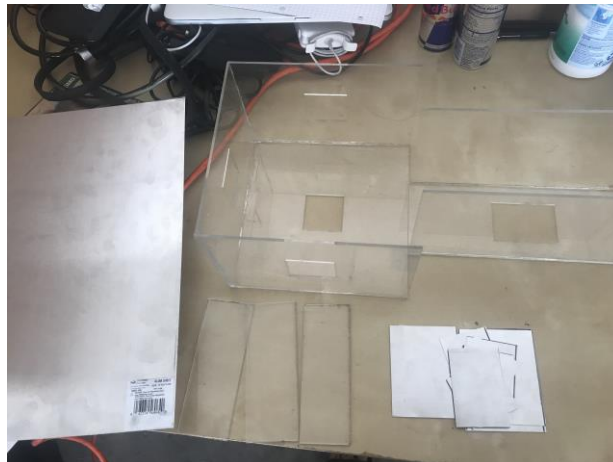


Figure 22. Final Prototype Assembly: Picture of parts of the final prototype as well as the process of assembling the acrylic pieces.

Prototype Assembly

When assembling the tank, the square and the rectangular portion were built simultaneously but separately. First, we made sure to wipe the acrylic sheet with a wet-wipe to remove dirt and dust. Then, a sandpaper was used on the edges to increase the friction coefficient and increase the adhesiveness of the epoxy. The acrylic panes were held using right angle fixtures and let dry for approximately five to ten minutes.

Once the square and rectangle of the tank dries, the extra panes to seal the two parts are glued using epoxy. Once all acrylic parts are pieced together, the aluminum sheets are glued to the acrylic. There are a total of five square aluminum cuts and one rectangular cut for the electrode placements. After the metal pieces were dried and set, two rectangular pieces of acrylic were placed on the insides of the square as a fixture for the square lid of the tank. The square lid was machined to be about 1cm shorter in width and length of the square base.

Test Protocol Development

Tank Test Protocol

When we began developing the manufacturing protocol for the tank design, we developed a few tests that we considered to be crucial to the stability and performance of the tank as a long-term fixture. These tests included a leak test, saline validation test, and a pressure validation test which can be found in appendix E. The leak test was designed to ensure that throughout any length of experimentation, the tank would be able to contain the saline solution without leakage at any point. Using tap water, we initially determined that our choice of epoxy was correct along with our method for joining the panels of acrylic. However, during the integration tests we quickly realized that the saline solution was causing the epoxy to erode resulting in leakage from the tank. After changing the epoxy to a solution developed for marine applications, we ensured that further leak tests were performed with the saline solution rather than tap water. The data from the leak tests were recorded by location and number of leaks per iteration. We developed a saline validation test for individuals who require an exact impedance measurement when performing experiments with the EnSite system. Due to the requirements of our project set forth by our sponsor, we did not need to record impedance data while performing integration tests, but future research may require these data. After we demonstrated successful bonds between the epoxy and acrylic panels with zero leaks, we performed pressure tests on the first tank to determine a baseline for testing the integrity of future tanks. If the future tests could withstand the max pressure that caused failure of the first tank, there was a significant inclination that the new tank's integrity would not fail. The pressure test was designed to ensure that the tank would be able to withstand the pressure from normal experimentation conditions and was performed after the epoxy was completely cured. For both pressure tests, we tested for max

weight for fracture and any flexion of the tank's panels. The weight was increased by 1kg for both vertical and horizontal tests and any cracks or leaks were noted. For the horizontal pressure test, we placed the tank with one of the side panels faced down and applied a determined weight on the center of the panel that was directly above. Once all the weights were tested, the tank was returned to its normal position and a vertical pressure test was performed by placing cardboard across the top of the tank and centering the weights above the center of the main tank chamber. The data recorded from this test was a note of any flexion or fracture of epoxy bonds between acrylic panels that would suggest a possible leak.

Integration Validation Protocol

The protocol we developed for validating the integration was modified throughout the project to account for the obstacles and limitations that occurred. Initially the protocol was based solely off of the instructions for use for the system and ensured that every necessary step was included. While these steps may be crucial to success in a clinical setting, they require adaptation for a laboratory setting. The initial protocol included all the system components and connections that would be required in a clinical setting but there were a few components that were not necessary such as those to record and store EKG data. The protocol we adapted starts with proper setup requirements for system components, the surface electrodes, the reference patch, necessary catheters, and the patient reference sensors. Once all these components are in place, the user can then perform the built-in validation action. Given our inability to utilize the CathLink Module pin block for diagnostic catheters, the protocol defines the necessary steps needed to collect geometry and map with the TactiCath SE ablation catheter. As mentioned previously, the TactiCath will have its limitations when collecting geometric data points

throughout the model creation process due to its limited number of electrodes. If the lab were to receive the pin block, the user could create these models using diagnostic catheters that contain more electrodes per spline using the same method of model creation once the specifications of the catheter have been added to the system.

We decided to include the EnSite NavX Navigation and Visualization Technology setup and model creation guide in this protocol because performing the system validation process is required each time a new study is performed. The visualization setup and model creation portion of the protocol became what we used for our final integration validation verification and the setup for the final study to demonstrate the capabilities of the integration. When we started the project, we had a goal of performing a series of tests that would validate the system integration and also conduct a study that would demonstrate the accuracy of the integration. The series of tests that we wanted to conduct for an accuracy demonstration included comparing collected geometry to actual measurements and a point of reference test with the catheter. The goal of the geometry test was to collect geometries of various materials at different impedance levels and temperatures and compare them to the actual measurements of the objects. For the point of reference tests, we wanted to establish a three-dimensional space within the NavX system, designate a reference point within that space, then measure the distance between the catheter tip location and the reference point. We would have also incorporated other distance tests such as measuring the distance between two objects and performed all these tests under the various environments set in the geometry collection tests. The final study we initially designed analyzed lesion depth and diameter from an ablation with a constant temperature and contact force when the sample is resting in the different environments that we established. Throughout the year we

adjusted these tests to account for the lack of equipment, assistance, and support that was a result of COVID-19 rules and restrictions.

The final integration validation test protocol we developed became the final study that would be used to demonstrate the capabilities of the system. We used a TactiCath SE ablation catheter to perform these tests and since we only had 1 available catheter, we had to design the protocol to be done in a single trial. The tests we performed collected the geometry of a few items of different materials in a defined environment that represented the average normal impedance/salinity of the human heart. The materials we wanted to test with were wood, acrylic, rubber, and glass. After consulting Abbott personnel, we decided that running these tests under different salinity environments would not yield statistically significant differences because the system is designed to adapt to changes in impedance throughout the procedure. The geometry we collected was isolated and measured using the built-in tools within the NavX software and these measurements were compared to the actual measurements. We created the geometries of a glass bowl, a rubber toy, and the inside of the tank itself. During experimentation we discovered that we could not perform any tests with wood inside the testing area. We later learned that if we wanted to perform tests on wood, we would need to transform it into a conductor at a low voltage through means of complete water saturation. Wood is naturally resistive in the order of 1017 ohm-ern at room temperature (Skaar, 1988). To use wood for modeling or testing, it would also require enough space in any cavity that the catheter is roving to allow enough of the saline solution to exist on all sides of the catheter. The testing apparatus we designed out of wood contained very small cavities, essentially the size of the catheter in use, therefore the system was not able to determine the location of the catheter. The wood being resistive and acting as an insulator for the 8 kHz signal being propagated from the patch electrodes resulted in signals

being dampened and mostly blocked from reaching the catheter electrodes. Another discovery we made during the experiment was that our range of working space was limited to essentially the area above the left/right and neck surface electrodes. We gathered as many points as possible on one side of the tank in an attempt to determine a measurable working area and the limitations of where data points can be collected. After consulting Abbott personnel, it was determined that the working motion box begins approximately 10cm above the magnetic field frame. This confirms the measurements we made when determining the workable area within our tank.

Testing Data and Analyses

Test	Leak Locations
1	4
2	2
3	0

Trials	Weight	Observations
1	6.35 kg	Horizontal: Minimal flex/ no cracks Vertical: No flex/cracks
2	7.1 kg	Horizontal: Flex, small cracks Vertical: No flex/cracks
3	8.5 kg	Horizontal: Flex, small cracks Vertical: Flex, epoxy failed

Table 3 and 4 contains the results of the tests performed on our first prototype, which was the original octagonal design. The leak test was performed using tap water to fill the tank completely to determine if there were any areas of weakness within the bonding of panels. After 10 minutes of water resting in the tank, each bond was assessed to identify any leaks. After the first trial, we discovered 4 leaks that required another application of epoxy. After the epoxy was completely cured, a second trial was run and resulted in 2 leaks in a different location. The leaks

occurring in a different location may be due to damage from moving the tank while pouring out the solution or simply because those bonds were weakened as the exposure time to water increased. Increased water exposure time continuously saturates the epoxy casing absorption that may lead to leaks if the bond between the epoxy and acrylic is insufficient or too thin. After the 2 areas of weakness were treated, a third test was run and resulted in zero leaks. This third test allowed us to determine the best methods of epoxy application that we would use for creating our next prototypes. We originally wanted to use minimal amounts of epoxy to join each of the acrylic panels for aesthetic purposes. To do so, we only applied epoxy along the thin width of the panel and used the application tool to wipe away excess epoxy that formed once the panels were joined with pressure. We determined after our failed attempts the aesthetics were relatively insignificant. Therefore, we decided to apply epoxy along each of the fused seams on the inside of the tank and used the application tool to ensure that the epoxy was evenly displaced and completely covered the seams. The first trial of the horizontal pressure test contained a weight of 6.35 kg being placed which resulted in minimal flex in the panels. After allowing it to sit for 10 minutes, the weight was removed, and the tank was inspected for any cracks in the panels or bonds. After confirming there was no damage, the tank was returned to its horizontal state and the next weight of 7.1 kg was placed on the panels. During this trial, the tank's panels experienced flexion and small cracks of the epoxy-acrylic bond were audibly noticed. Once there was confirmation that there was not any significant damage, we proceeded with the 8.5 kg weight. Significant damage was characterized as any cracks or damage that would lead to saline leaks due to panel separation. During that trial, flexion was noticed during the horizontal pressure tests, but no additional cracks were observed. While performing the vertical pressure test, the epoxy-acrylic bond failed on the left side of the main chamber within seconds of placing

the weight, therefore determining our max load until failure. We used the results from these pressure tests along with the results from the final leak test to determine a baseline for testing future prototypes. Since we had zero leaks by the end of the testing trials for the first prototype, we needed to ensure that future tanks must be able to withstand at least a weight of 8.5 kg in both directions.

Table 5: Second Prototype Leak Test	
Cups of Saline Solution	Leak Locations
18	0
22	0
26	0
30	0
34	0

Table 6: Second Prototype Pressure Tests		
Trials	Weight	Observations
1	6.35 kg	Horizontal: No flex/cracks Vertical: No flex/cracks
2	7.1 kg	Horizontal: No flex/cracks Vertical: No flex/cracks
3	8.5 kg	Horizontal: Flex, no cracks Vertical: No flex/cracks

Table 5 and 6 contains the results of the tests performed on our second prototype, the new squared tank design with aluminum patches on each side where a surface electrode is placed. When we initially filled this tank with a saline solution to verify our epoxy application, we noticed that the solution was leaking through the epoxy bonds between panels. After doing some research, we discovered the epoxy we were using was not rated for marine applications therefore was being eroded by the salt. After sealing the tank with a marine epoxy, we ran leak tests with saline solution to determine any weaknesses in the bonds. The initial trial was run with 18 cups of the solution sitting in the tank for 10 minutes upon which the tank was examined for leaks. There were no visible leaks, so we added 4 more cups of the solution and observed after 10 minutes. This process was repeated until 34 cups of saline solution were poured into the tank. After every trial, it was determined that there were no visible leaks at any location of the tank confirming that the application and epoxy type were correct. The pressure test performed on the horizontal axis resulted in no cracks at any weight but there was flexion noticed when applying the 8.5 kg weight. The vertical test resulted in no cracks or flexion throughout all 3 weights tested. This confirmed that the tank was able to withstand the maximum weights that caused the first prototype to fail.

Table 7: Final Prototype Leak Tests	
Cups of Saline Solution	Leak Locations
18	0
22	0
26	0
32	0
36	0

Table 8: Final Prototype Pressure Tests		
Trials	Weight	Observations
1	6.35 kg	Horizontal: No flex/cracks Vertical: No flex/cracks
2	7.1 kg	Horizontal: No flex/cracks Vertical: No flex/cracks
3	8.5 kg (MAX)	Horizontal: No flex/cracks Vertical: No flex/cracks

Table 7 and 8 contains the results of the tests performed on our final prototype which incorporated all the tank modifications that we developed from the previous designs. The leak tests were performed the same as with the second prototype but with an increased volume of saline solution per trial. After completing all trials of the leak test with the defined number of cups, it was determined that there were no visible leaks due to weakness in the bonding of the

panels. We then performed the pressure tests exactly as we did with the previous prototypes. After performing each trial with the defined weights, we determined that there were zero breaks and no noticeable deformations in the panels.

Table 9: Integration Validation Attempts		
Integration Attempt	Result	Configuration/Setup
1	Fail	Tank, magnet, and necessary components placed on a metal table. Surface electrode patches were placed on acrylic walls as shown in Figure 23A.
2	Fail	Tank, magnet, and necessary components placed on a plastic table. Salinity of solution was increased from previous attempt.
3	Fail	Tank, magnet, and necessary components placed on a plastic table. Surface electrode patches were placed on aluminum integrated into the walls and system reference patch placed on acrylic in new configuration as shown in Figure 23B.
4	Success	Tank, magnet, and necessary components placed on a plastic table. Surface electrode patches and system reference patch were placed on aluminum integrated into the walls and configured as shown in Figure 23B.

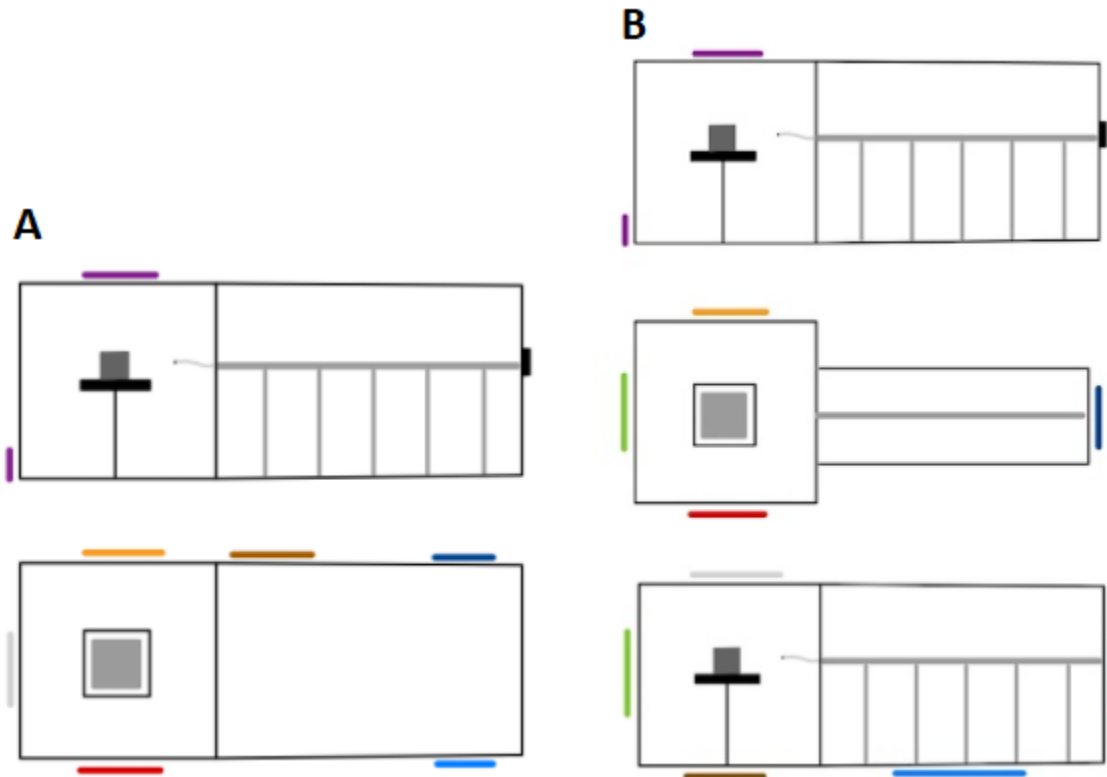


Figure 23: A) Configuration of surface electrode patches, PRS patches, and system reference patch used for integration attempts 1 and 2. B) Configuration of all patches used in integration attempts 3 and 4.

After confirming that the tank was strong enough to withstand the forces of being completely filled with saline solution, we began our integration validation attempts. Table 9 displays the results of all 4 attempts to validate the integration between the tank and the EnSite Precision mapping system. Once all the patches and sensors were placed according to the protocol, we used the NavX software built in validation tool to validate the integration. After failing attempt 1, we implemented some possible solutions which included increasing the salinity and replacing the metal table with a mainly plastic table. The swapping of the table was a result of the system detecting a significant amount of metal distortion causing disruption in signal acquisition. Attempt 2 yielded the same failure so we were able to rule our salinity as the reason

for initial failure and focused on the patch placement. We reached out to a clinical specialist at Abbott who suggested we rearrange the patches to the configuration in Figure 23 B. It was also determined that the surface electrode patches were unable to emit the 8 kHz signal through the acrylic after reaching out to Dr. Hawkins, so we integrated aluminum squares in the area where each patch was located to use as a conductive medium between the surface electrodes and the saline solution. We attempted and failed to validate the integration during our 3rd attempt but realized through the generated system error messages that our issue was with the system reference patch not being placed on an aluminum patch like the surface electrodes were. After attaching the system reference patch to the conductive medium, we attempted a 4th trial which resulted in a successful system validation. The validation confirmed a successful integration between the wet lab and the Ensite Precision system. We kept all external components (patches, sensors) in the same location and performed the system validation process numerous times to ensure we did achieve a successful integration.

We performed a study after successfully validating that tested the accuracy and limitations of the integration. This study used a TactiCath SE ablation catheter along with the NavX software to gather data points along the inner surface of various objects in an attempt to create a virtual model of those objects. The geometry generated by the system was measured using the built-in tool and compared to the actual measurements of the objects. For the glass bowl, one side of it was modeled and measured horizontally for analysis. This model yielded the most accurate results of all the objects tested with only a 11.70% error with a 13.56mm absolute error. Absolute error describes the difference between the actual and measured values in units of millimeters. Percentage error is the degree to which the measurements of the models differed as a

proportion to the actual measurement of the physical model. We believe the reason for this low error percentage is because this object contained thin walls, had an open end that allowed more current by saline solution to flow through, and the glass itself was not resistive to current. The second object used was a bone shaped rubber toy that was cut in half to create an open-ended side for the catheter. We noticed that collecting data points on this object was significantly more difficult than the glass bowl which was demonstrated by the 24.18% error with a 20.73 mm absolute error when measuring the length and a 19.52% error with a 5.58 mm absolute error when measuring the proximal width of the opening of the object. We were unable to achieve the shape of the bone at the due to the lack of data points gathered by the system. We believe interference and the physical properties of rubber are what prevented us from gathering an accurate geometric model. As we mentioned previously, we discovered that essentially the bottom half of the tank was unable to be used for testing since the software could not recognize it as a workable area. We needed to elevate the rubber object into the working area, and we believe that the objects used to hold up the object were causing significant interference blocking the signals sent out by surface electrodes. The interference combined with rubber's natural tendency to resist conductivity and prevent electrons from moving freely are the reasons it was difficult for the system to collect data points at the distal end of the object. The final object we collected data points on was the acrylic tank itself. The reasons we chose this item were both to see how well the system detects the surface of an acrylic panel as well as to determine the limitations of the working zone. After creating geometry from the data points, the horizontal measurement from the system was 14.19% different from the actual measurement of the tank with a 31mm absolute error. This error percentage is not ideal in regard to accuracy, but it is what we expect to achieve based on the location of the where we were collecting data points. The wall of the acrylic tank

that we collected data points contains the left surface electrode patch. We theorized that we would not yield very accurate results on that wall because the catheter was too close to the aluminum patch that is emitting the 8 kHz current from the electrode. The system provides visualization of the catheter based on the location of the electrodes in the impedance field. When the catheter was on the same wall as the left patch, the system could not utilize that surface electrode to interpret where the catheter electrodes were within the field because there was virtually no distance of separation between the electrodes and the patch.

Table 10: Study Measurements					
Object	System Measurement (mm)	Average Sys. Measurement (mm)	Physical Measurement (mm)	Absolute Error (mm)	Percent Error
Glass Bowl	103	102.33	115.89	13.56	11.70 %
	103				
	101				
Rubber Toy	Length: 61	65	85.73	20.73	24.18 %
	Length: 70				
	Length: 64				
	Proximal Width: 23	23	28.58	5.58	19.52 %
	Proximal Width: 22				
	Proximal Width: 24				
Acrylic Tank	184	183	214	31	14.49 %
	181				
	181				
	181				
	188				

Discussion and Future Directions

The objective of this thesis project was to develop a functioning wet lab that integrates with the EnSite Cardiac Mapping system that currently resides in the St. Jude research lab at Cal Poly for future students, faculty, and industry personnel to perform experiments and demonstrations for academic purposes. When we initially began designing our tank, we took the advice of clinical experts regarding the ideal shape of the tank. We started with a hexagonal and an octagonal shaped chamber with the intention of placing all of the surface electrode patches on each wall to completely surround the object resting in the testing chamber. After some research and advice from lab technicians that have experience with wet labs, specifically ones that are designed for this system, we identified that these shapes and placement of the patches were not going to work the way we needed to. We determined that a tank that contained a squared testing chamber and a long rectangular portion on the bottom end of the tank was necessary to ensure that all the patches could be placed with the appropriate amount of spacing relative to each other. While testing the integrity of our tanks through the leak and pressure tests, the most noteworthy change we made to the manufacturing of all our prototypes was to account for the salinity in the solution by how it affects the epoxy that bonds the panels together. We initially performed the leak tests with tap water and were able to determine the best application methods for the epoxy based on the locations of the leaks. However, when we filled the tank with the saline solution for integration attempts, we discovered that the longer we left the solution in the tank, the more leaks that would occur. After some examination and assistance from a local expert, we discovered that the epoxy we were using was eroding away due to long term contact with the saline solution. From that point on we ensured that any epoxy or sealant we used was rated for marine applications and that future leak tests would be done using saline rather than simply tap water.

After completing the integrity tests on our second prototype, we began our integration validation attempts. When we failed our first attempt at a successful integration, we considered that the impedance from the saline solution was not high enough for the surface electrodes to pass current through and possibly an incorrect placement of the patches. We decided to restart the validation protocol with a higher concentration of saline while keeping the patches in the same place as a control but still did not achieve a successful integration. We tried moving the patches around and even ensured that the system was set up correctly by placing the patches on our body and simulating a patient in a clinical setting. Once we verified that the setup and the saline concentration were correct, we decided to reach out to Abbott specialists to see why the patches were not integrating with our wet lab. While consulting the specialist, we first determined that the placement of our patches was not correct because the patches needed to be placed in certain axes in order for the system to create a x-y-z impedance field in the workable area. After some discussion with trial and error with our third attempt, we concluded that each patch required a conductive medium that connects it to the saline solution directly, so we installed aluminum patches where each surface electrode and the system reference patch needed to be. The aluminum squares needed to be large enough, so it covers the entire surface electrode patch and most of the system reference patch surface. Once all the modifications were in place and the ideal saline concentration was achieved, the software successfully validated the integration between the wet lab and the mapping system.

The experimental study we conducted demonstrated that the integration allows users to create models by collecting geometric data points within a reasonable accuracy given our circumstances. Due to supply limitations and the inability to receive the proper hardware, we were limited to gathering geometries with the TactiCath SE ablation catheter only rather than the

appropriate diagnostic catheters designed for mapping. As previously mentioned, when using a linear multi electrode catheter with the EnSite Precision system, users can yield up to 94% accuracy when collecting geometric data points to create models. The TactiCath SE having only 4 electrodes with 2-2-2 spacing allows the collection of geometric data but only 2 points can be captured at a time resulting in low density models. The density of models in this regard pertains to the amount of data points collected to build a geometric model and any kind of voltage map. Using diagnostic catheters that are manufactured to record several points at each save results in higher density maps, thus models and maps that are more accurate. During the study we noticed that the more objects that were in the tank causing interference, the more difficult it was for the system to collect data points in the areas of higher obstruction. When only the glass bowl sat in the tank with the open end facing the front patch, we achieved our lowest error percentage (11.7%) when comparing the virtual model to the physical measurement. When we stacked objects in an attempt to hold the rubber object within the workable area, the comparison resulted in very high error percentages of 19.52% when measuring the width of the opening and 24.18% when measuring the entire length of the object. The objects we used to hold up our physical model were unsaturated wood blocks that acted as insulators in the order of 1017 ohm-cm at room temperature for the alternating current being emitted by the surface electrode patches. The wooden blocks were placed directly above the “back” surface electrode in an attempt to have our physical model centered in our workable area. As previously mentioned, the system gathers geometric data points by detecting the location of catheter electrode bipoles within its generated impedance field. By placing the wooden blocks in between the object and that posterior surface patch, the system was unable to detect the location of the electrodes on the catheter from that posterior patch resulting in a lack of data points gathered with respect to the Z axis between the

two patches. The data points more distal from the opening of the object were difficult to gather due to this interference so they were very scarce in the total amount of points collected which is demonstrated by the high error percentage when measuring the length. Rubber's resistance to current by nature also played a significant role in the inability to gather accurate results. With the current setup and tank prototypes, users can collect the geometry of simple objects if there is minimal interference between the object and the surface electrodes. The best way to minimize the interference is to build a stand composed of non-insulating material, such as acrylic, that can serve as a permanent fixture for holding up objects of interest within the workable field.

Based on our data and the literature that suggests very high levels of accuracy when creating geometric models with the appropriate catheters and minimal interference inside the tank, users can expect measurement differences with less than 15% error which should be acceptable for most immediate applications and experimental ideas for this wet lab. For more clinical purposes, this error percentage tolerance should be significantly lower to due to the small measurements of most anatomical structures within the heart. As mentioned previously, when using a mapping system for procedures such as slow pathway modification for AVNRT, physicians can have 90-95% success rates from the system localizing the site for ablation. The location of the slow pathway is typically around 15mm away from the bundle of His. Having that 90-95% success means that not only is the slow pathway modified, but the bundle of His is not affected by the ablation. If the correct catheters are used in an environment with minimal interference for reasons previously discussed, users should expect the error percentages of their measurements to be very minimal. Professors or industry representatives can come in and perform academic demonstrations with the system that will allow them to explain the science and engineering

behind each of the components and demonstrate how the system generates models based on the built-in algorithms.

Going forward with the development and use of this Cath lab, prospective students, faculty, and industry personnel would focus on increasing the accuracy and workable area of the tank to perform more complex experiments and ablation procedures. As demonstrated with our testing data, we were able to collect data points using a TactiCath SE ablation catheter that the NavX software used to create geometric models. This is a significant step in the right direction when it comes to the future of this lab on Cal Poly's campus. One of the first suggestions we have for prospective users is to build a taller tank or increase the height of the stand at least 3 inches to increase the workable area to allow for testing and experimentation on larger objects. At the moment, the vertical workable area is approximately 3.9 inches from the top panel that contains the front surface electrode patch which leaves around 2.5 inches of a "dead zone" at the bottom of the tank. This significantly limits the size of objects that can be tested in our current tank prototypes because ideally the object will need to rest in the middle of the tank, not touching any panels. After reaching out to engineers at Abbott, we discovered that the workable area using magnetics in tandem with impedance is limited to a 35x35x30 cm three-dimensional motion box. This motion box has a 10cm "dead zone" that begins at the top of the Precision Field Frame magnet which is why we could not obtain any information or use the system to visualize our catheters when we were in that bottom portion of the tank. By increasing the height of the stand or building a tank tall enough to encompass the full workable motion box, future users can study larger objects inside the tank. Another alternative, though not recommended, is to disable the collection and use of SE (magnetic) data points while creating models or mapping voltage. By disabling the magnetic field and collection of SE points, the user can eliminate that dead zone

and proceed with collecting only impedance data. The reason we suggest not turning off magnetics is that the PRS-anterior sensor placed near the chest surface electrode patch functions as a sensor for metal distortion. One of the biggest issues we faced when trying to yield accurate models was not using a diagnostic catheter to collect data points. Although the TactiCath SE has the ability to create a model through collecting points, it is not the primary tool used to map and collect geometry in a clinical setting. The TactiCath SE's main function is to ablate areas of problematic electrical activity through contact force technology and serves as essentially a secondary tool when it comes to collecting data points. For future users to use diagnostic catheters to create models, the Cath lab will require the CathLink pin module from Abbott to plug in all the necessary pins. Using diagnostic catheters, especially the Advisor HD Grid Mapping Catheter, will yield the most accurate results under optimal conditions. With this catheter users can map more complex geometries along with gathering data that ablation catheters simply are not designed for.

If the lab is to be used for a more academic/demonstration purpose, we suggest purchasing an artificial heart in the form of ballistic gel or another conductive material. Like Abbott's educational labs, prospective students could build a tank that permanently houses the artificial heart with built-in tubes that guides catheters into the chambers of the heart from the rectangular portion of the tank. This will allow the demonstrator easy access each time they collect geometry on the model heart in the tank. One prospective idea to demonstrate the limitations of traditional bipolar catheters in comparison to the HD Grid or to simply study the propagations of different arrhythmias is to create a waveform generator. This generator can be composed of many smaller electrodes that are programmed to emit a signal at different times thus creating various patterns. This would be beneficial for prospective students who are

developing catheters or sheaths to test their product's ability to read voltage patterns. With the current components in the lab, future users can study ablation techniques, compare ablation catheters, or even simply demonstrate how ablation procedures are performed in a clinical setting. The lab contains the Ampere equipment that generates radio frequency energy and a Cool Point pump that can be used for irrigated catheters. Users can perform ablations using irrigated and non-irrigated, contact force and standard catheters on meat or chicken to analyze lesion depth and effectiveness for studies or in-services. The status and setup of the Cath lab we developed allows users to practice validation/tank/saline protocols, gather simple geometries, and perform ablation procedures. With a few more hardware components mentioned previously, users have the potential to build a fully functional wet lab capable of many academic and clinical purposes. We have demonstrated that the current integration between our tank design and the EnSite Precision cardiac mapping system is not only valid, but also of practical use for future students, faculty, and industry personnel.

References

- Abbott. (n.d.). *About advisor HD grid*. Abbott.
<https://www.cardiovascular.abbott/us/en/hcp/products/electrophysiology/diagnostic-catheters/advisor-hd-grid.html>.
- Abbott. (n.d.). *How the TactiCath Contact Force ablation catheter, SE works*. How the TactiCath Contact Force Ablation Catheter, SE Works.
<https://www.cardiovascular.abbott/us/en/hcp/products/electrophysiology/ablation-technology/tacticath-se-ablation-catheter/about/how-it-works.html>.
- Ali, M., Padmanabhan, D., Kanjwal, K., Ghadei, M. K., Kottayan, A., Banavalikar, B., & Shenthur, J. (2021). Effect of fluoroscopy frame rate on radiation exposure and in-hospital outcomes in three-dimensional electroanatomic mapping guided procedures. *Journal of arrhythmia*, 37(1), 97–102. <https://doi.org/10.1002/joa3.12496>
- Alfonso-Almazán, J. M. (2019). Lesion index titration using contact-force technology enables safe and effective radiofrequency lesion creation at the root of the aorta and pulmonary artery. *Circulation: Arrhythmia and Electrophysiology*, 12(3).
<https://doi.org/10.1161/circep.118.007080>
- Alonso Pedrote, Eduardo Arana-Rueda, Lorena García-Riesco, Adriano Jiménez-Velasco, Juan Sánchez-Brotons, José M. Arizón-Muñoz, José M. Fernández-Pérez, Manuel Frutos-López. Three-Dimensional Impedance Mapping as an Aid to Circumferential Pulmonary Vein Isolation in Paroxysmal Atrial Fibrillation, Volume 62, Issue 3, 2009, Pages 315-319, ISSN 1885-5857, [https://doi.org/10.1016/S1885-5857\(09\)71563-4](https://doi.org/10.1016/S1885-5857(09)71563-4).
- Baton Rouge General. (2019, May 9). *New treatment for AFIB reduces stroke risk*. Baton Rouge General. <https://www.brgeneral.org/news-blog/2019/may/new-treatment-for-afib-reduces-stroke-risk/>.
- Berte, B., Zeppenfeld, K., & Tung, R. (2020). Impact of Micro-, Mini- and Multi-Electrode Mapping on Ventricular Substrate Characterisation. *Arrhythmia & electrophysiology review*, 9(3), 128–135. <https://doi.org/10.15420/aer.2020.24>
- Buescher, T., Traci L. Buesche Asirvatham, S., Samuel J. Asirvatham, & Asirvatham, C. (2010, December 01). Three-Dimensional Mapping of Cardiac Arrhythmias.
- Boles, U., Gul, E. E., Fitzpatrick, N., Enriquez, A., Conroy, J., Ghassemian, A., David, S., Baranchuk, A., Simpson, C., Redfearn, D., Glover, B., Abdollah, H., & Michael, K. (2017, June 15). *Lesion size index in maximum voltage-guided CAVOTRICUSPID ablation for atrial*

flutter. The Journal of innovations in cardiac rhythm management.
<https://www.ncbi.nlm.nih.gov/pmc/articles/PMC7252914/>.

Borlich, M., Iden, L., Kuhnhardt, K., Paetsch, I., Hindricks, G., & Sommer, P. (2018). 3D Mapping for PVI- Geometry, Image Integration and Incorporation of Contact Force Into Work Flow. *Journal of atrial fibrillation*, 10(6),

Bryant, R. M., Allshouse, K., & Markert, C. (2021). Uncovering "bipolar blindness" with high-density orthogonal mapping at the scar-related critical isthmus in repaired congenitally corrected transposition of the great arteries. *HeartRhythm case reports*, 7(5), 328–332.
<https://doi.org/10.1016/j.hrcre.2021.02.007>

Cho, H.-O. (2015). Radiation Dose and Cancer Risk of Cardiac Electrophysiology Procedures. *International Journal of Arrhythmia* , 16(1), 4–10.

Choudhuri, I. (2016, August 12). *Principles and techniques of cardiac catheter mapping*. Thoracic Key. <https://thoracickey.com/principles-and-techniques-of-cardiac-catheter-mapping/>.

D. C. Deno, H. J. Sih, S. P. Miller, L. R. Teplitzky and R. Kuenzi (March 2014). "Measurement of Electrical Coupling Between Cardiac Ablation Catheters and Tissue," in IEEE Transactions on Biomedical Engineering, vol. 61, no. 3, pp. 765-774, doi: 10.1109/TBME.2013.2289328.

Dave, J. K. (2016, September). *Why is the X-ray tube usually located ... - ajronline.org*.
<https://www.ajronline.org/doi/pdfplus/10.2214/AJR.16.16454>.

De Ponti R. (2015). Reduction of radiation exposure in catheter ablation of atrial fibrillation: Lesson learned. *World journal of cardiology*, 7(8), 442–448.
<https://doi.org/10.4330/wjc.v7.i8.442>

Deno , D. C. (2014). *Measurement of electrical coupling between cardiac ablation catheters and tissue*. IEEE transactions on bio-medical engineering. Retrieved October 29, 2021, from <https://pubmed.ncbi.nlm.nih.gov/24235298/>.

EMCO Industrial Plastics. (n.d.). FAQs for acrylic. Emco Plastics.
<https://www.emcoplastics.com/acrylic-faqs/>.

Ferry D.R.(Ed.). (2007). Reentrant arrhythmias.*ECG in 10 Days*. McGraw Hill.
<https://accesscardiology.mhmedical.com/content.aspx?bookid=1839§ionid=128106343>

FDA. (n.d.). *Fluoroscopy: FDA*. U.S. Food and Drug Administration.
<https://www.fda.gov/radiation-emitting-products/medical-x-ray->

imaging/fluoroscopy#:~:text=Fluoroscopy%20is%20a%20type%20of,is%20passed%20through%20the%20body.

Gupta, A. K., Maheshwari, A., Thakur, R., & Lokhandwala, Y. Y. (2002, January 1). Cardiac mapping: Utility or futility? *Cardiac Mapping: Utility or Futility?* <https://www.ncbi.nlm.nih.gov/pmc/articles/PMC1569897/>.

Giaccardi, M., Mascia, G., Paoletti Perini, A., & Giomi, A. (2018, June 12). Long-term outcomes after "Zero X-ray" arrhythmia ablation. Long-term outcomes after "Zero X-ray" arrhythmia ablation. <https://link.springer.com/article/10.1007/s10840-018-0390-7>.

Haber, T., Kleister, G., & Selman, B. (2016, June 30). Interactive in-vitro training in physics of radiofrequency ablation for physicians and medical engineering students. *Interactive In-Vitro Training In Physics Of Radiofrequency Ablation For Physicians And Medical Engineering Students*. <https://www.ncbi.nlm.nih.gov/pmc/articles/PMC5089504/>.

Hong K, Glover B17 The use of half concentration saline is superior for the catheter ablation of typical atrial flutter *Heart* 2019;105:A15.

Issa, Z. F., Miller, J. M., & Zipes, D. P. (2009, December 4). *Mapping and navigation modalities*. *Clinical Arrhythmology and Electrophysiology* (1). <https://www.sciencedirect.com/science/article/pii/B9781416059981000069>.

Jais P, Shah DC, Haissaguerre M, et al. Efficacy and safety of septal and left-atrial linear ablation for atrial fibrillation. *Am J Cardiol*. 1999; 84: 139R–146R.

Johnson, J. C., Thaul, S., & Mettler, F. A. (1997). *Evaluation of Radiation Exposure Guidance for Military Operations: Interim Report (Compass series)*. National Academies Press.

Joseph, J.P., Rajappan, K., Radiofrequency ablation of cardiac arrhythmias: past, present and future, *QJM: An International Journal of Medicine*, Volume 105, Issue 4, April 2012, Pages 303–314, <https://doi.org/10.1093/qjmed/hcr189>

Koruth, J.S., Heist, E.K., Danik, S. *et al*. Accuracy of left atrial anatomical maps acquired with a multielectrode catheter during catheter ablation for atrial fibrillation. *J Interv Card Electrophysiol* 32, 45 (2011). <https://doi.org/10.1007/s10840-011-9573-1>

Koutalas, E. (2015, March 10). *Contemporary mapping techniques of complex cardiac arrhythmias - identifying and modifying the arrhythmogenic substrate*. *Arrhythmia & electrophysiology review*. <https://pubmed.ncbi.nlm.nih.gov/26835095/>.

Leshem, E., Tschabrunn, C. M., Jang, J., Whitaker, J., Zilberman, I., Beeckler, C., Govari, A., Kautzner, J., Peichl, P., Nezafat, R., & Anter, E. (2017). High-resolution mapping of

ventricular scar. *JACC: Clinical Electrophysiology*, 3(3), 220–231.
<https://doi.org/10.1016/j.jacep.2016.12.016>

Mantovan, R. (2006). *Anatomical and electrophysiological approach to atrial fibrillation ablation: Technical limitations*. *Journal of cardiovascular medicine* (Hagerstown, Md.). Retrieved October 29, 2021, from <https://pubmed.ncbi.nlm.nih.gov/16858236/>.

Morillo, C. A., Banerjee, A., Perel, P., Wood, D., & Jouven, X. (2017). Atrial fibrillation: the current epidemic. *Journal of geriatric cardiology : JGC*, 14(3), 195–203.

Natale A, Reddy VY, Monir G, Wilber DJ, Lindsay BD, McElderry HT, Kantipudi C, Mansour MC, Melby DP, Packer DL, Nakagawa H, Zhang B, Stagg RB, Boo LM, Marchlinski FE. *Paroxysmal AF catheter ablation with a contact force sensing catheter: results of the prospective, multicenter SMART-AF trial*. *J Am Coll Cardiol*. 2014 Aug 19;64(7):647-56. doi: 10.1016/j.jacc.2014.04.072. PMID: 25125294.

Odutayo A, Wong C X, Hsiao A J, Hopewell S, Altman D G, Emdin C A et al.(2016) Atrial fibrillation and risks of cardiovascular disease, renal disease, and death: systematic review and meta-analysis *BMJ* 2016; 354 :i4482 doi:10.1136/bmj.i4482

Proietti, R., Dowd, R., Gee, L.V. et al. Impact of a high-density grid catheter on long-term outcomes for structural heart disease ventricular tachycardia ablation. *J Interv Card Electrophysiol* (2021). <https://doi.org/10.1007/s10840-020-00918-4>

Protechnix. (n.d.). Software Development Process Models.
https://www.pro-technix.com/services/software/models_evolution_frame.html.

Romero, J. (2015, November 12). *Electroanatomic mapping systems (carto/ensite navx) vs. conventional mapping for ablation procedures in a training program*. *Journal of interventional cardiac electrophysiology : an international journal of arrhythmias and pacing*. <https://pubmed.ncbi.nlm.nih.gov/26560500/>.

Schnabel R, Pecun L, Engler D, Lucerna M, Sellal JM, Ojeda FM, De Caterina R, Kirchhof P. *Atrial fibrillation patterns are associated with arrhythmia progression and clinical outcomes*. *Heart*. 2018 Oct;104(19):1608-1614. doi: 10.1136/heartjnl-2017-312569. Epub 2018 Mar 17. PMID: 29550771.

Shenasa, M., & Al-Ahmad, A. (2019). *Advances in cardiac mapping and catheter ablation*. Elsevier.

Skaar, C. (1988). *Electrical Properties of Wood*. Springer.
https://link.springer.com/chapter/10.1007/978-3-642-73683-4_6.

Stanford Health Care. (2019, May 14). *Arrhythmia Types*. Stanford Health Care (SHC) - Stanford Medical Center. <https://stanfordhealthcare.org/medical-conditions/blood-heart-circulation/arrhythmia/types.html>.

Tedrow, U. B. (2020, December 10). *Technology update for mapping, imaging, and ablation*. US Cardiology Review (USC). <https://www.uscjournal.com/articles/technology-update-mapping-imaging-and-ablation>.

Tschabrunn, C. M., Roujol, S., Dorman, N. C., Nezafat, R., Josephson, M. E., & Anter, E. (2016). High-Resolution Mapping of Ventricular Scar: Comparison Between Single and Multielectrode Catheters. *Circulation. Arrhythmia and electrophysiology*, 9(6), 10.1161/CIRCEP.115.003841 e003841. <https://doi.org/10.1161/CIRCEP.115.003841>

UCLA. (n.d.). *Arrhythmia, Sudden cardiac death & Ion channel biology*. UCLA Cardiovascular Research Theme. Retrieved October 29, 2021, from <https://medschool.ucla.edu/arrhythmia-sudden-cardiac-death-ion-channel-biology>.

Vañó E, Arranz L, Sastre JM, Moro C, Ledo A, Gárate MT, Minguez I. Dosimetric and radiation protection considerations based on some cases of patient skin injuries in interventional cardiology. *Br J Radiol*. 1998 May;71(845):510-6. doi: 10.1259/bjr.71.845.9691896. PMID: 9691896.

Veneri, L., Rossi, F., Botto, N., Andreassi, M. G., Salcone, N., Emad, A., Lazzeri, M., Gori, C., Vano, E., & Picano, E. (2009). Cancer risk from professional exposure in staff working in cardiac catheterization laboratory: insights from the National Research Council's Biological Effects of Ionizing Radiation VII Report. *American heart journal*, 157(1), 118–124.
<https://doi.org/10.1016/j.ahj.2008.08.009>

Vittorio Calzolari, Luca De Mattia, Stefano Indiani, Martino Crosato, Alberto Furlanetto, Claudia Licciardello, Paolo Antonio Maria Squasi, Zoran Olivari, In Vitro Validation of the Lesion Size Index to Predict Lesion Width and Depth After Irrigated Radiofrequency Ablation in a Porcine Model, *JACC: Clinical Electrophysiology*,

Viswanathan , K. (2016, November 17). *Evaluation of a novel high-resolution mapping system for catheter ablation of ventricular arrhythmias.*

<https://pubmed.ncbi.nlm.nih.gov/27867071/>.

Wade JP. Estimation of effective dose in diagnostic radiology from entrance surface dose and dose-area product measurements. *Br J Radiol.* 1998 Sep;71(849):994-5. doi: 10.1259/bjr.71.849.10195022. PMID: 10195022.

Weir, H. K. (2016). *Heart disease and cancer deaths - trends and projections in the United States, 1969-2020.* Preventing chronic disease. Retrieved October 29, 2021, from <https://pubmed.ncbi.nlm.nih.gov/27854420/>.

Appendices

Appendix A: Hydrostatic Force Calculation

$$\rho = 1.045 \frac{g}{mL} = 1045 \frac{kg}{m^3}$$

$$L = 8.5 \text{ in} = 0.2159 \text{ m}$$

$$R = 6 \text{ in} = 0.1524 \text{ m}$$

$$P = F/A \rightarrow F = P \cdot A \quad P = \rho g y$$

$$F = \int dF = \int P dA$$

$$= \int \rho g y L dy$$

$$= \rho g y \int_{y=0}^{y=h} y dy \rightarrow F = \rho g L \frac{y^2}{2} \Big|_0^h$$

$$= \rho g L \frac{h^2}{2} \rightarrow (1045 \frac{kg}{m^3}) (9.8 \frac{m}{s^2}) (0.2159 \text{ m})(0.1524 \text{ m})^2 * (1/2)$$

$$F = (1105.52)(0.1524)^2$$

$$= 25.677 \text{ N} \rightarrow 25.7 \text{ N}$$

Stresses @ Different Area Walls of the Cube

$$A_1 = 8.5 * 6 = 51 \text{ in} = 1.2954 \text{ m}^2$$

$$A_2 = 8.25 * 6 = 49.5 \text{ in} = 1.2573 \text{ m}^2 \text{ (max stress cube experiences)}$$

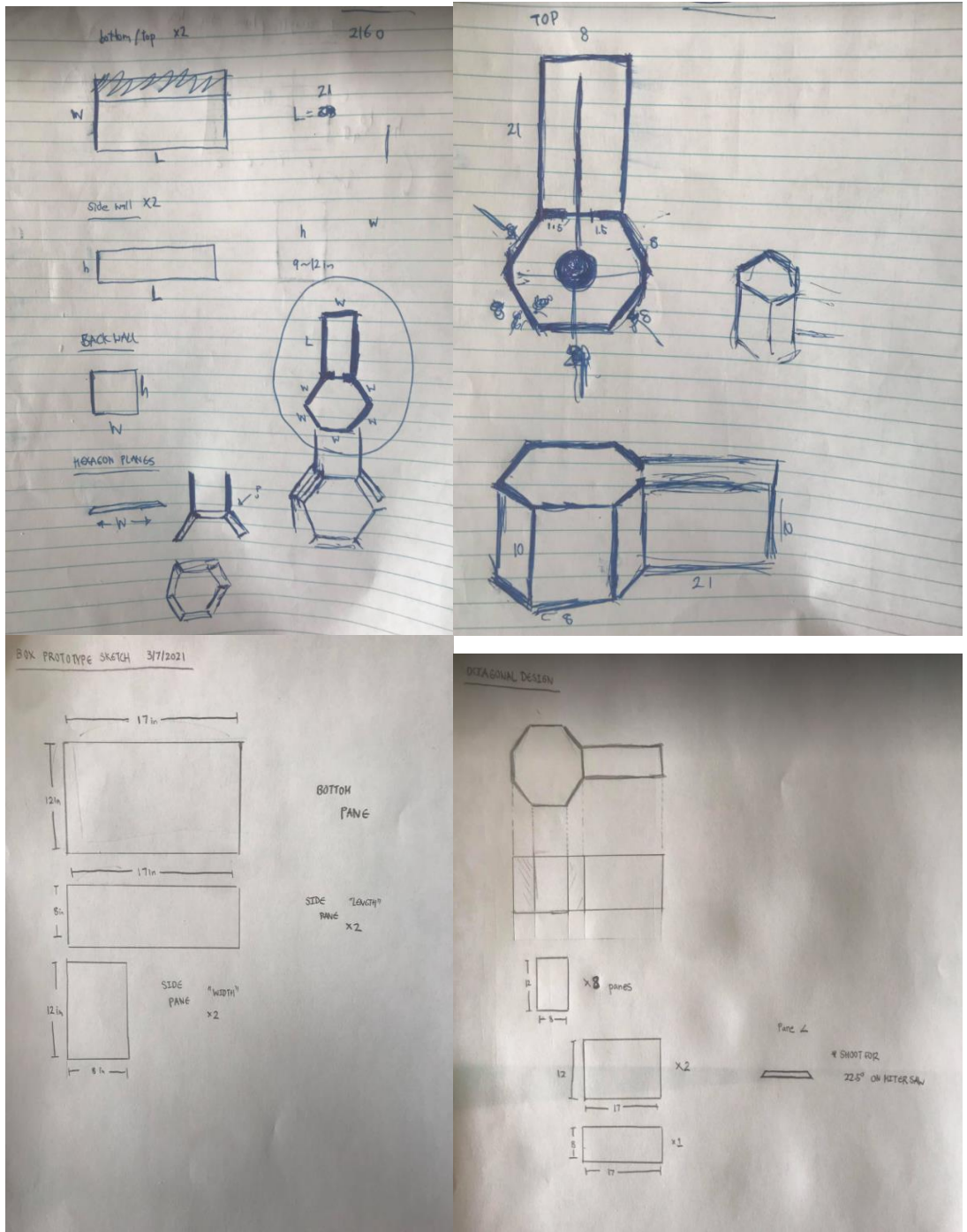
$$P_1 = \frac{F}{A_1} = \frac{25.7 \text{ N}}{1.2954 \text{ m}^2} = 19.84 \text{ Pa}$$

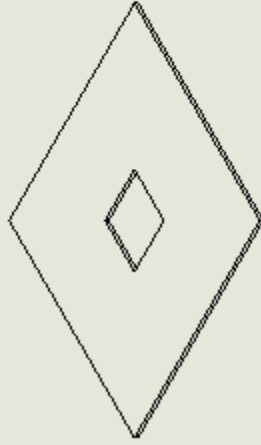
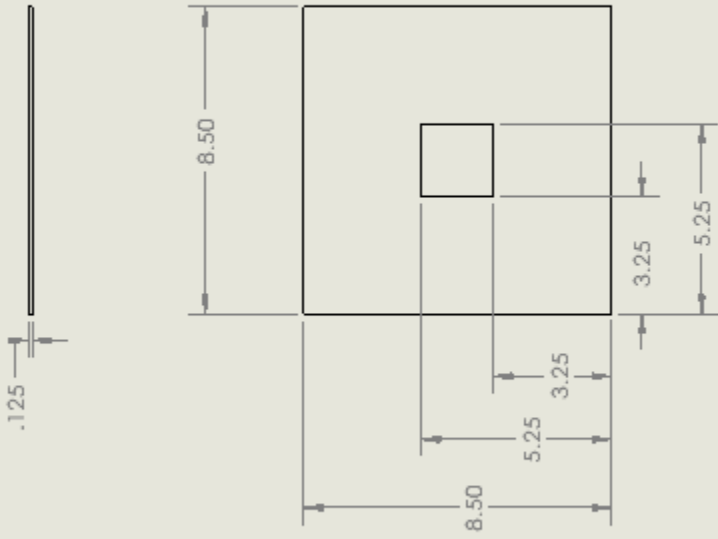
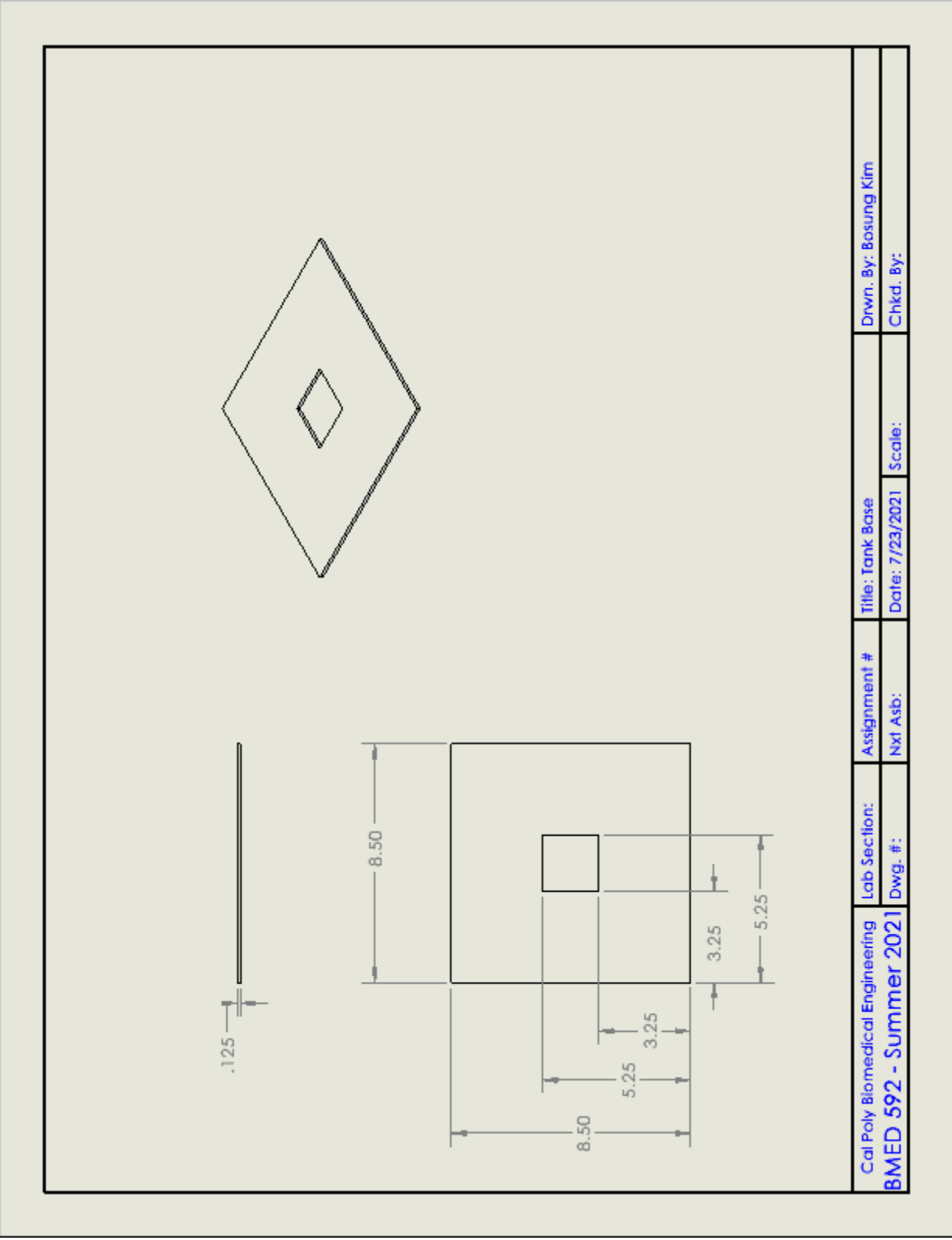
$$P_2 = \frac{F}{A_2} = \frac{25.7 \text{ N}}{1.2573 \text{ m}^2} = 20.44 \text{ Pa}$$

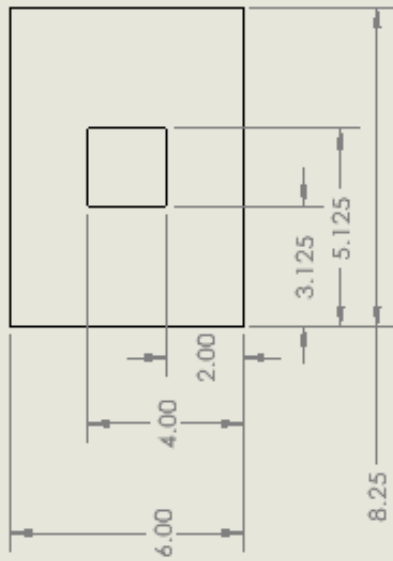
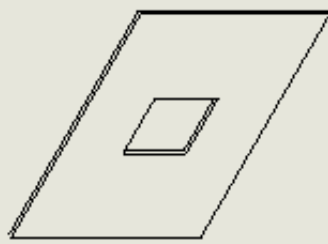
Appendix B: Table of Material Properties

Table 2: Mechanical Properties of Materials: Acrylic molded, cast, optical sheet, and plexiglass.				
	Acrylic (General Purpose, Molded)	Acrylic (Cast)	Acrylic (optical sheet)	Plexiglass (Arkema, V825)
Tensile Strength, Ultimate (MPa)	19.3-85 (Avg: 64.9)	62-83 (Avg: 74.4)	54-83 (Avg: 69.1)	70.3
Tensile Strength, Yield (MPa)	25- 85 (Avg: 60.5)	64.8- 83.4 (Avg: 75.4)	37.9-72 (Avg: 55.7)	N/A
Modulus of Elasticity (GPa)	0.950- 3.79 (Avg: 2.94)	2.76-3.30 (Avg: 3.10)	1.52-3.38 (Avg: 2.62)	3.10
Flexural Yield Strength (MPa)	33.1-143 (Avg: 103)	98-125 (Avg: 109)	57-120 (Avg: 101)	<=103 MPa
Compressive Yield Strength (MPa)	36.5- 117 (Avg: 102)	110-124 (Avg: 120)	117-124 (Avg: 119)	N/A

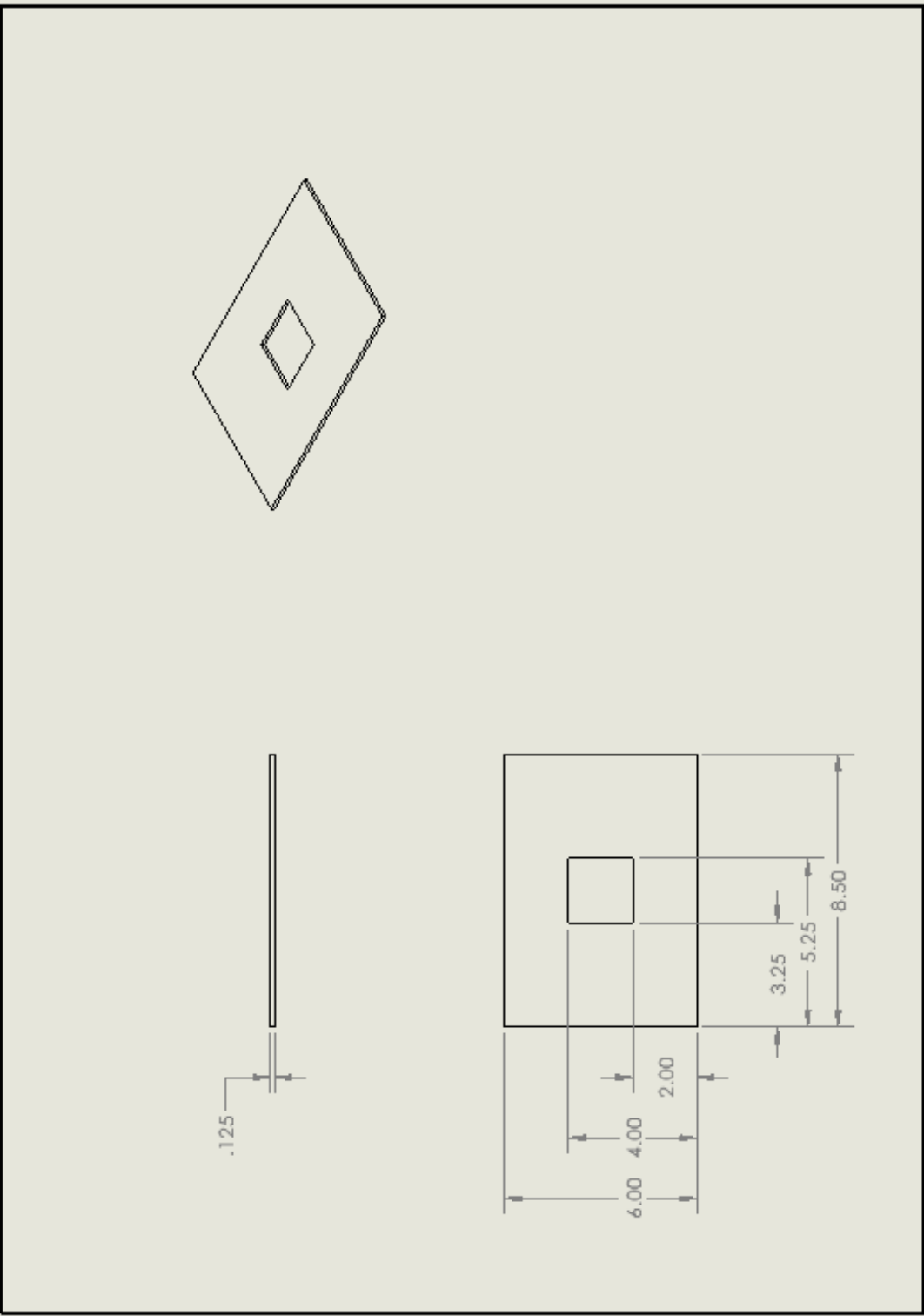
Appendix C: Detailed drawings and schematics



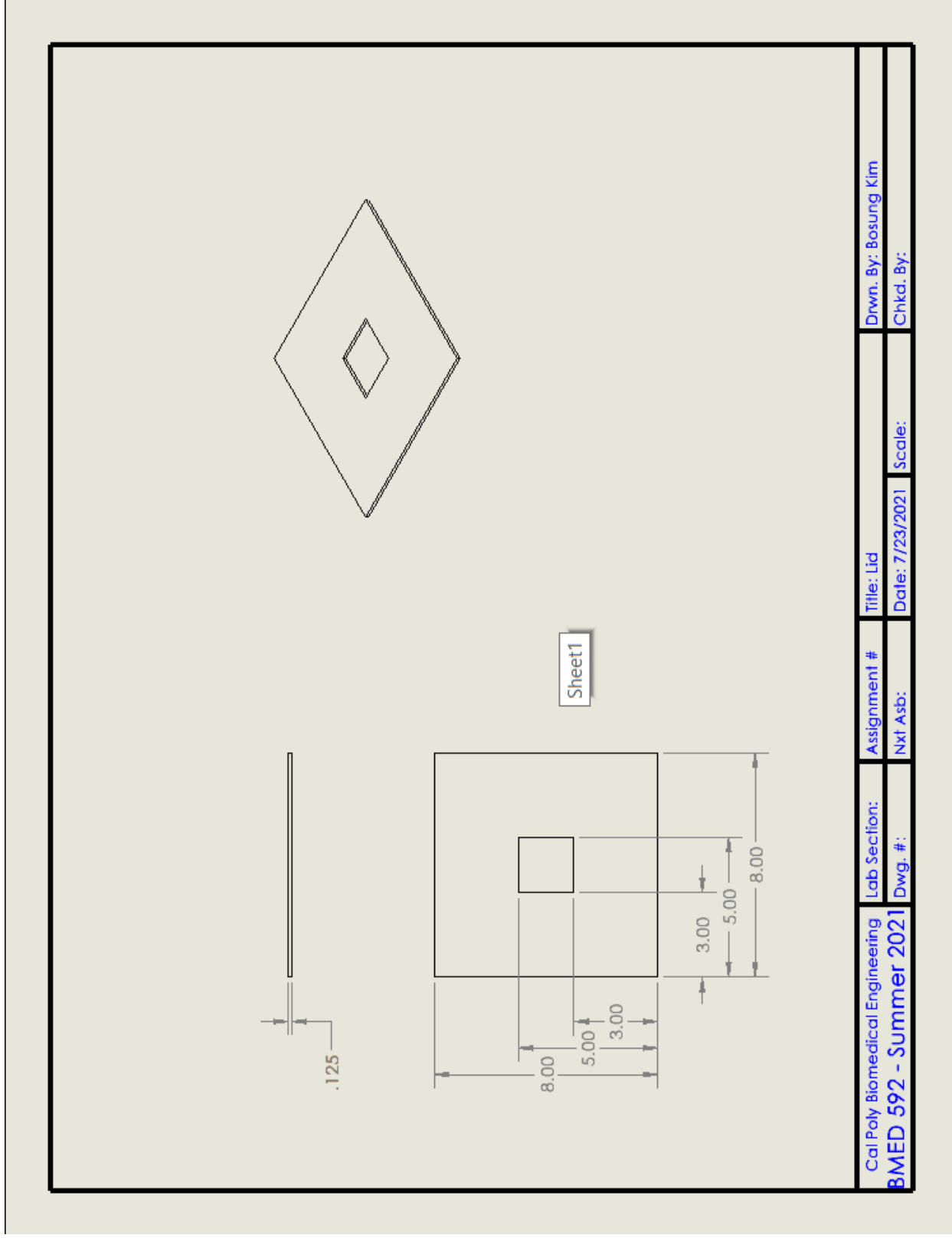


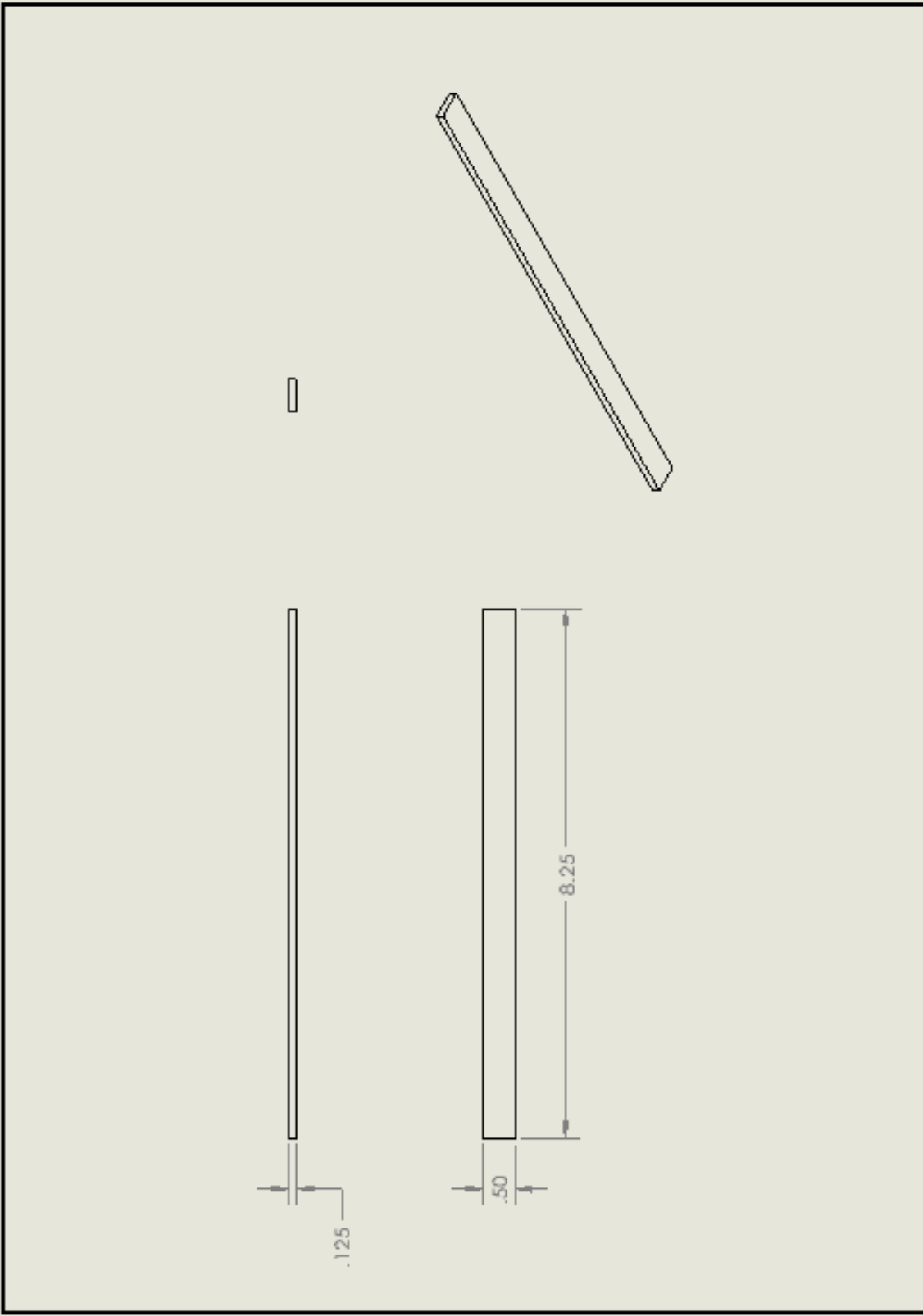


Cal Poly Biomedical Engineering	Lab Section:	Assignment #	Title: Front Pane	Drwn. By: Bosung Kim
BMED 592 - Summer 2021	Dwg. #:	Nxt Asb:	Date: 7/23/2021	Scale:
				Chkd. By:

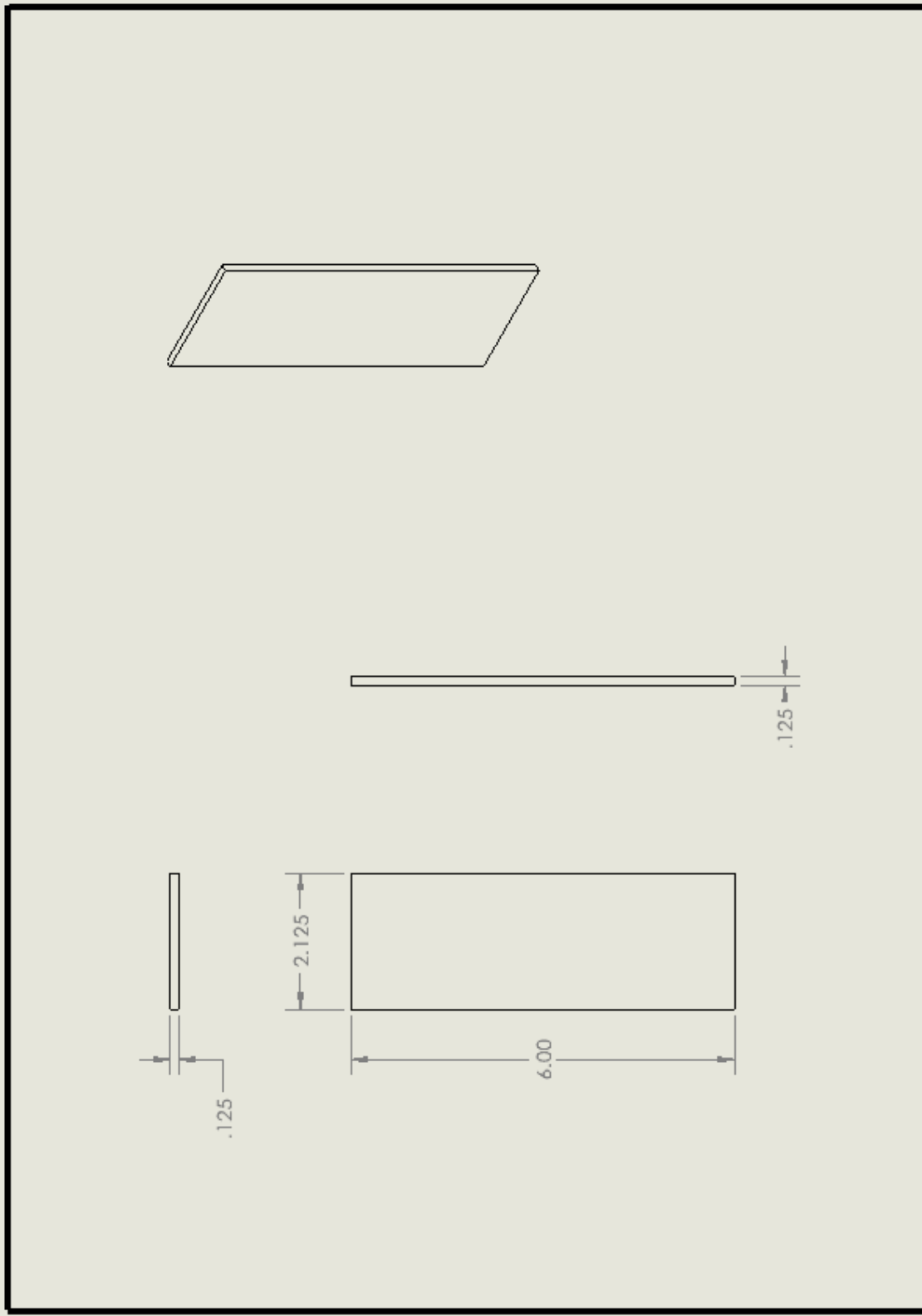


Cal Poly Biomedical Engineering	Lab Section:	Assignment #	Title: Left & Right Pane	Drwn. By: Bosung Kim
BMED 592 - Summer 2021	Dwg. #:	Nxt Asb:	Date: 7/23/2021	Chkd. By:

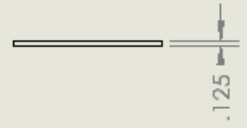
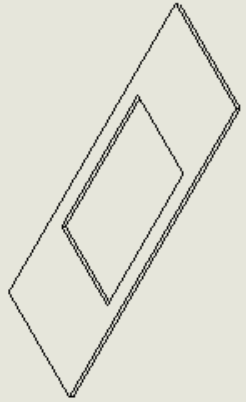
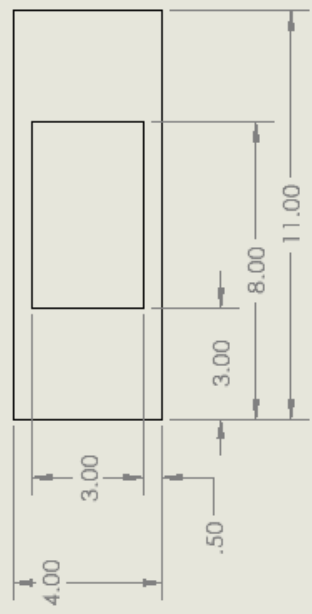
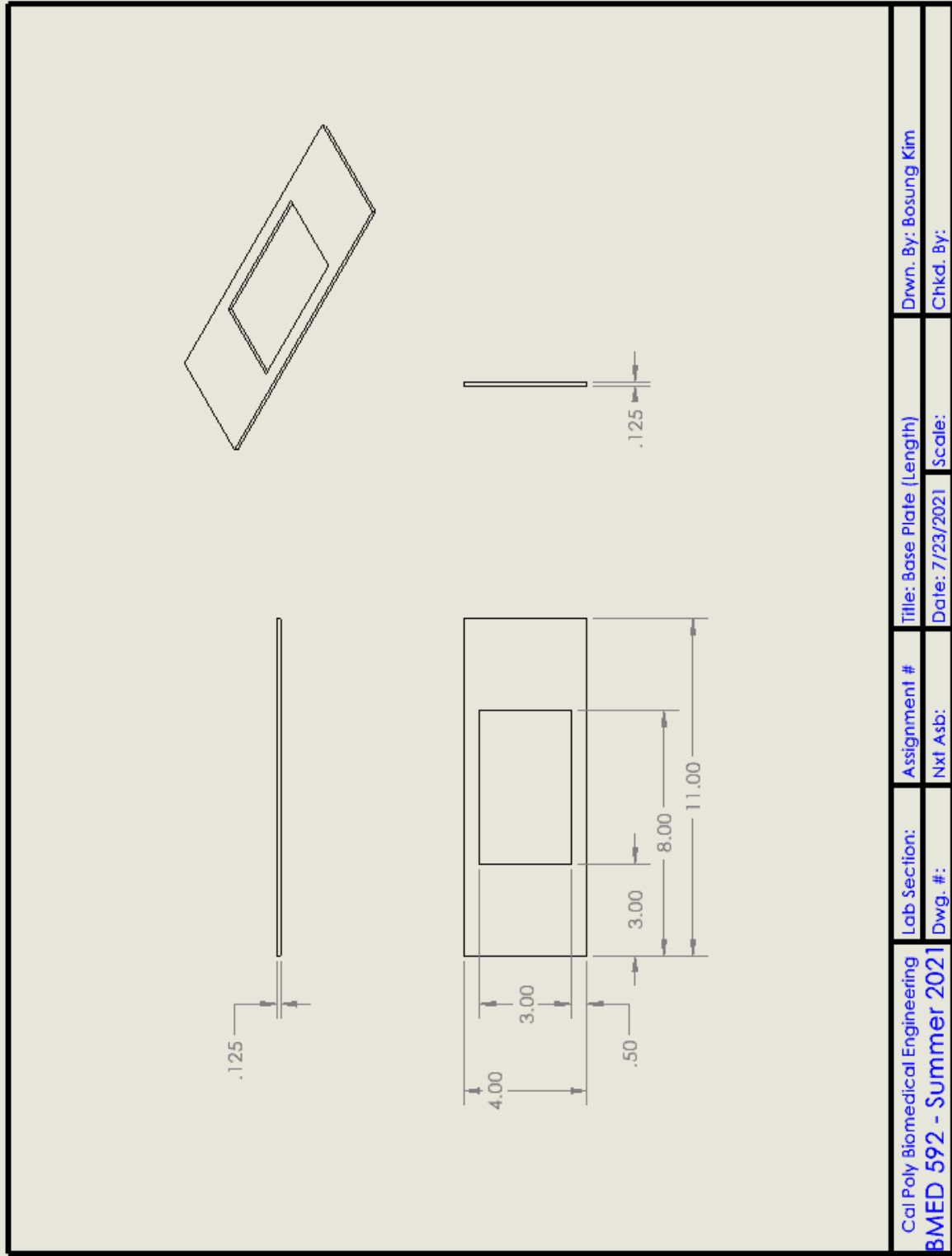


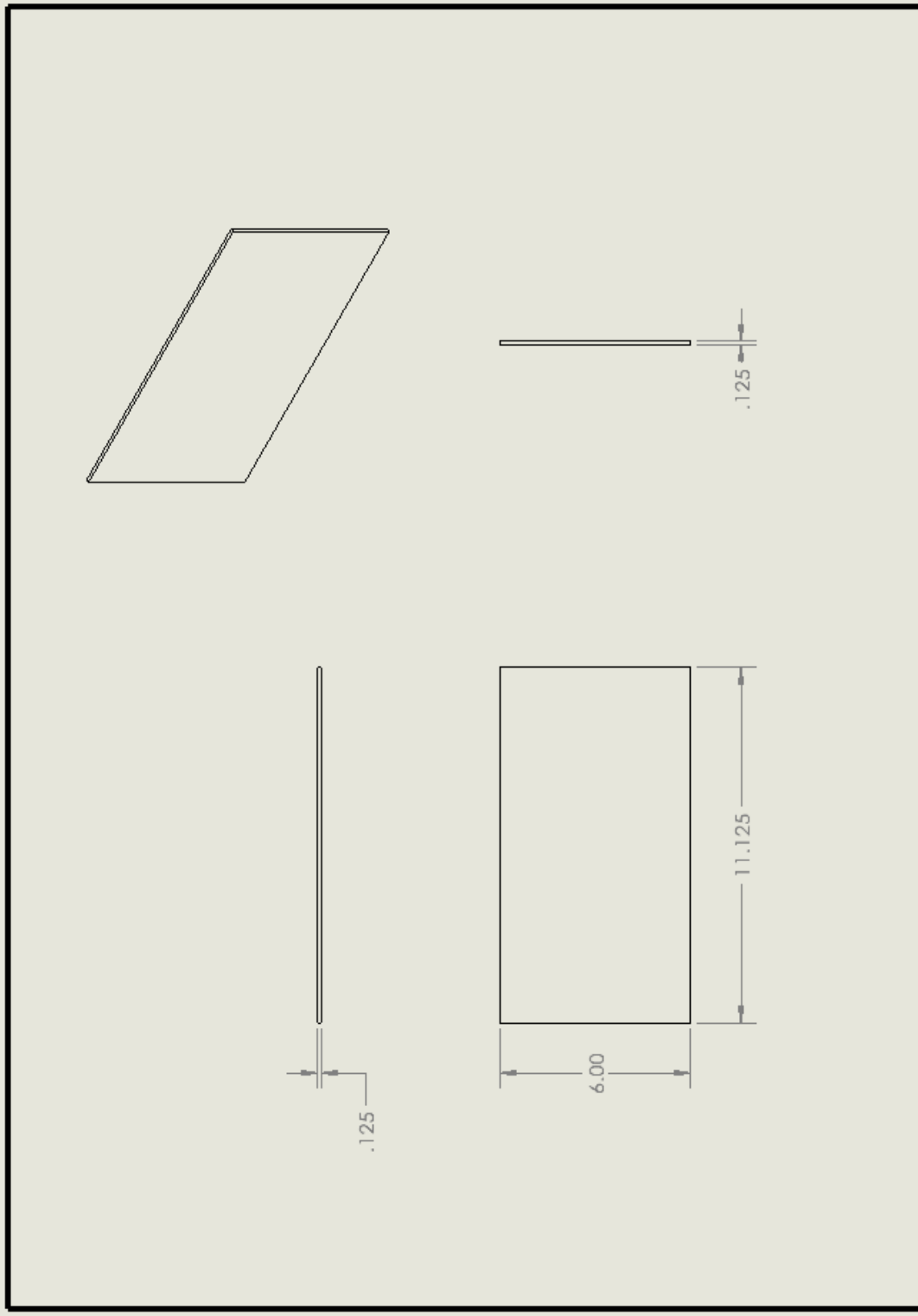


Cal Poly Biomedical Engineering	Lab Section:	Assignment #	Title: Lid Fixture	Drwn. By: Bosung Kim
BMED 592 - Summer 2021	Dwg. #:	Nxt Asb:	Date: 7/23/2021	Scale:
				Chkd. By:

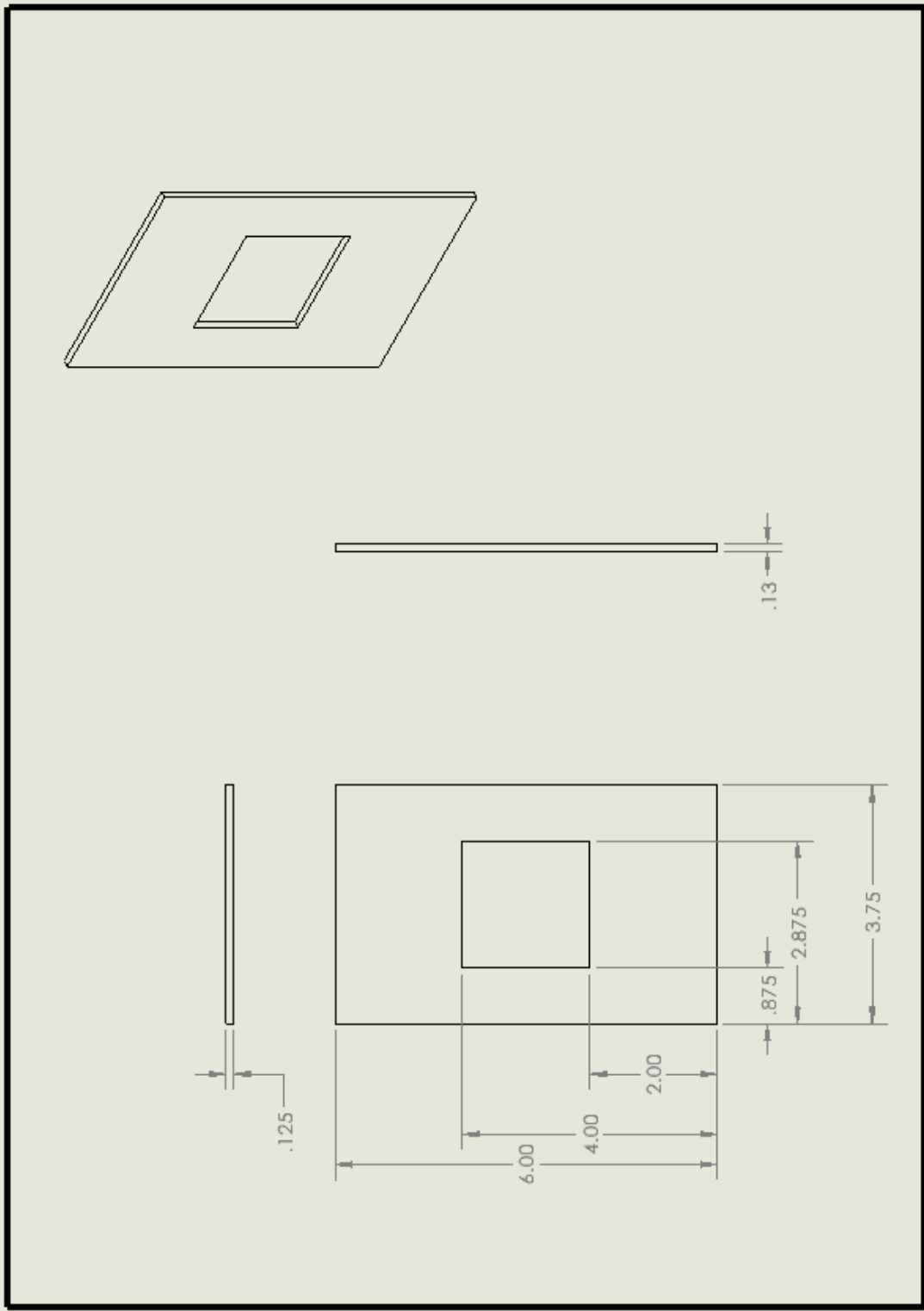


Cal Poly Biomedical Engineering	Lab Section:	Assignment #	Title: Side Pieces	Drwn. By: Bosung Kim
BMED 592 - Summer 2021	Dwg. #:	Next Assb:	Date: 7/23/2021	Scale:
				Chkd. By:



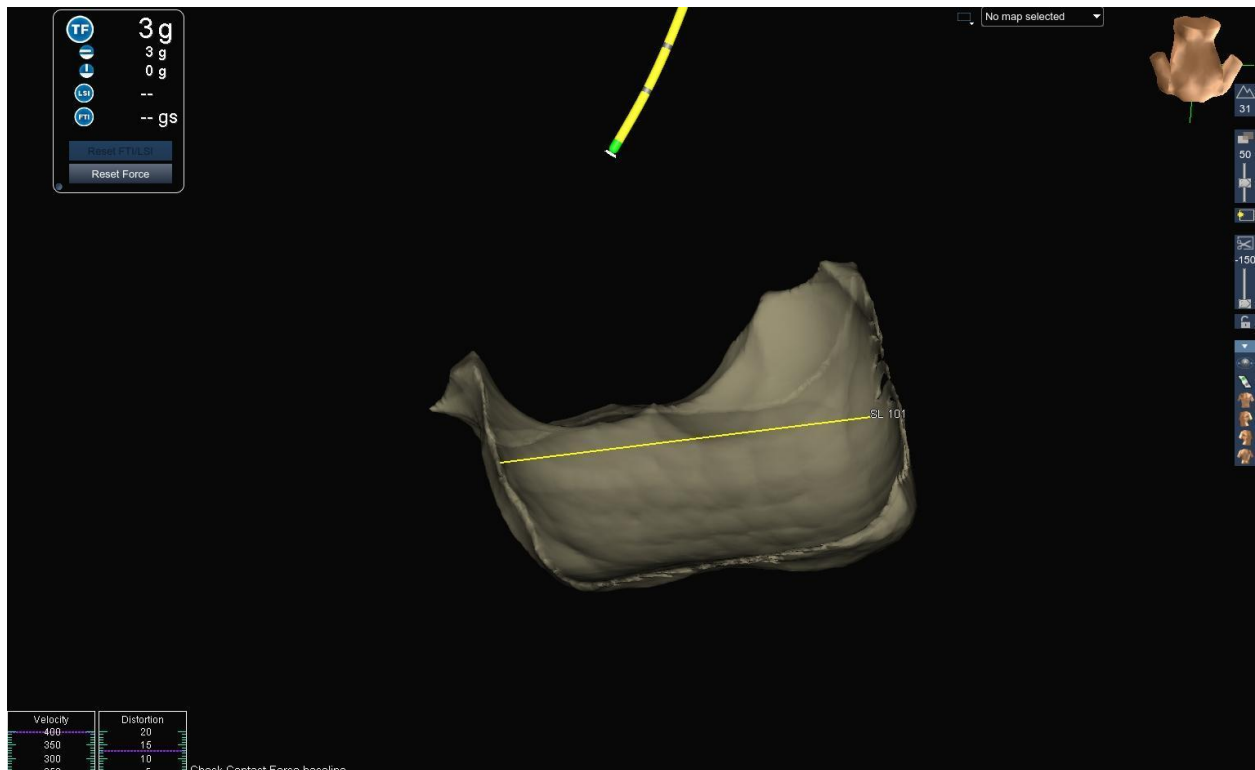
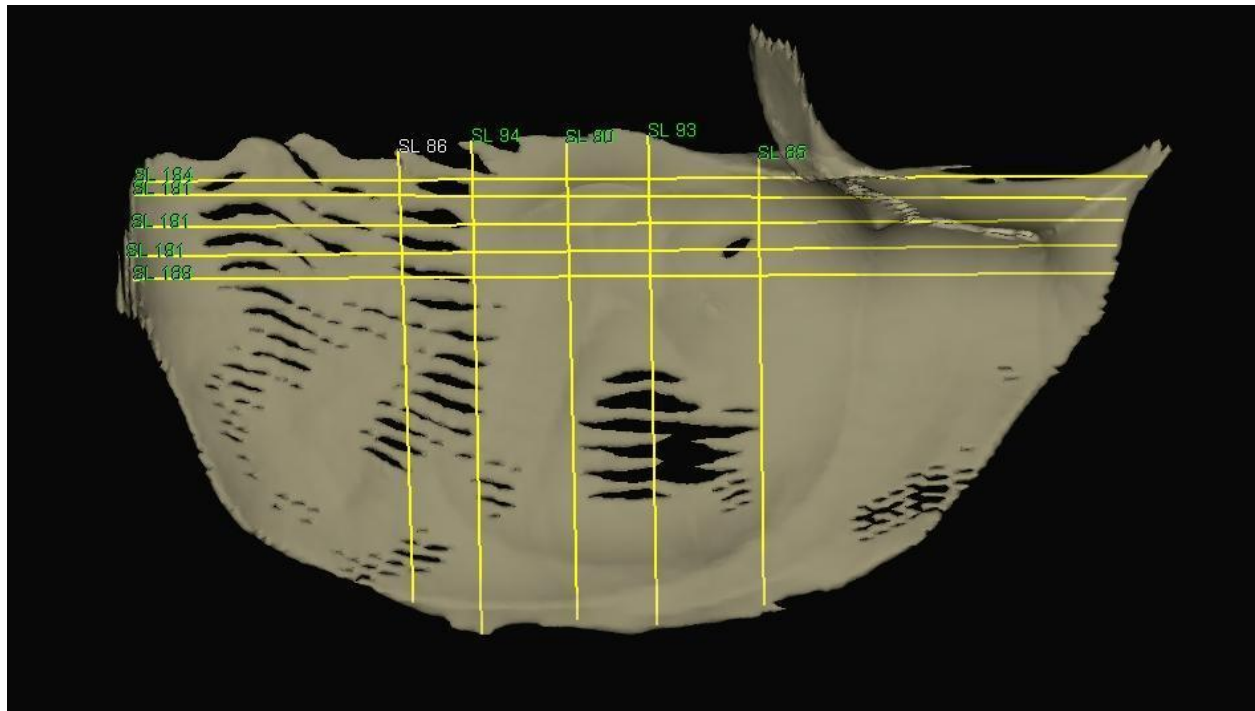


Cal Poly Biomedical Engineering	Lab Section:	Assignment #	Title: Left&Right Pane (Length)	Drwn. By: Bosung Kim
BMED 592 - Summer 2021	Dwg. #:	Nxt Asb:	Date: 7/23/2021	Chkd. By:

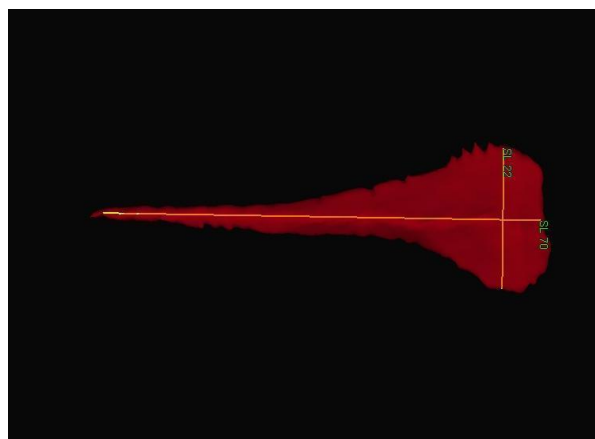
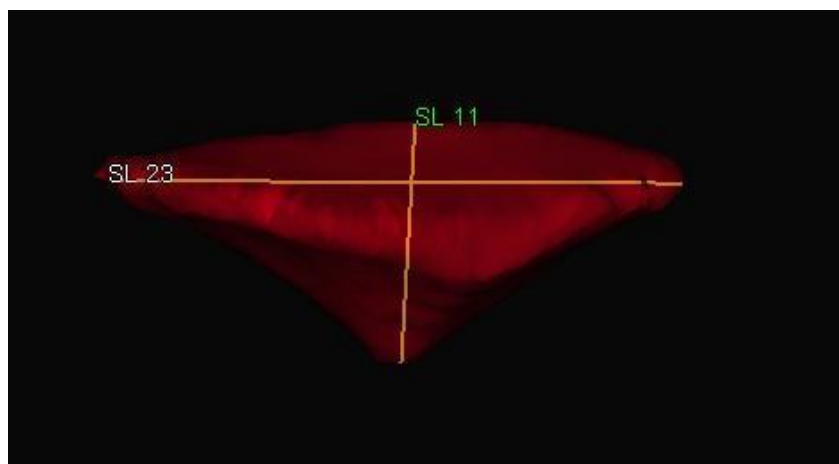
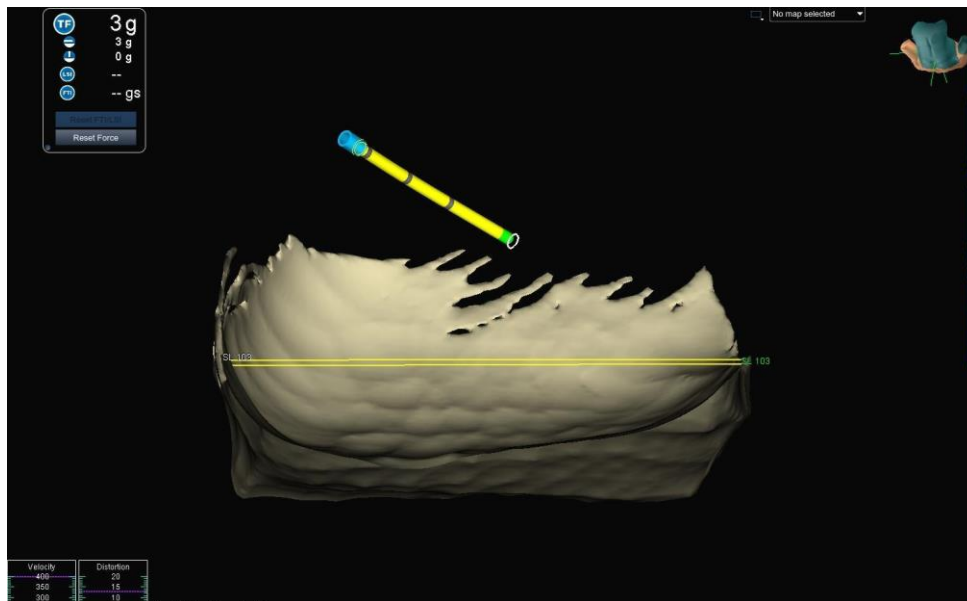


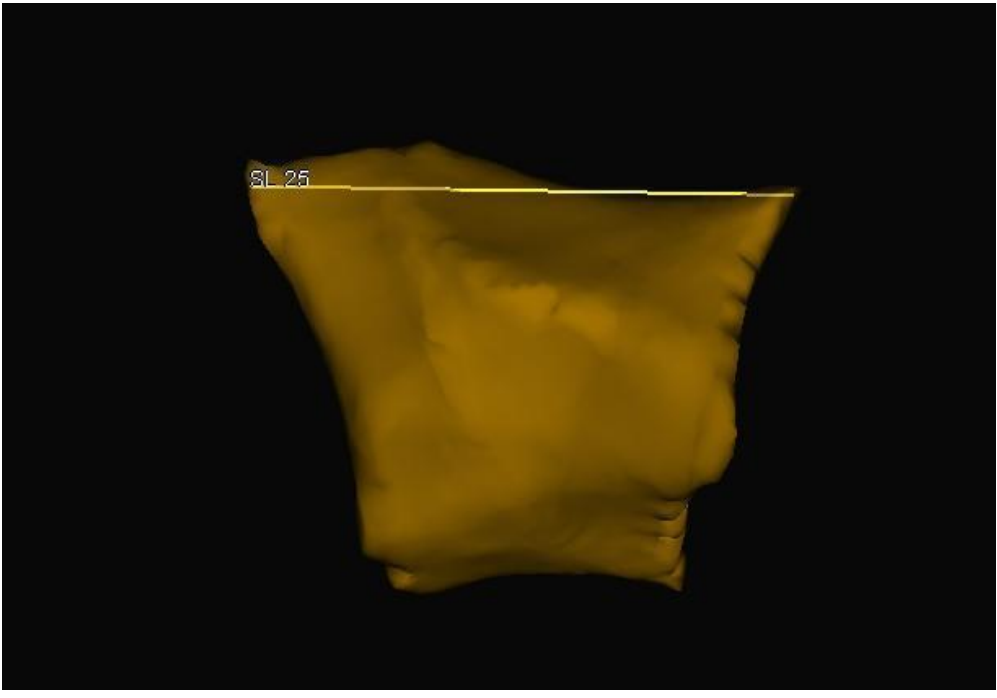
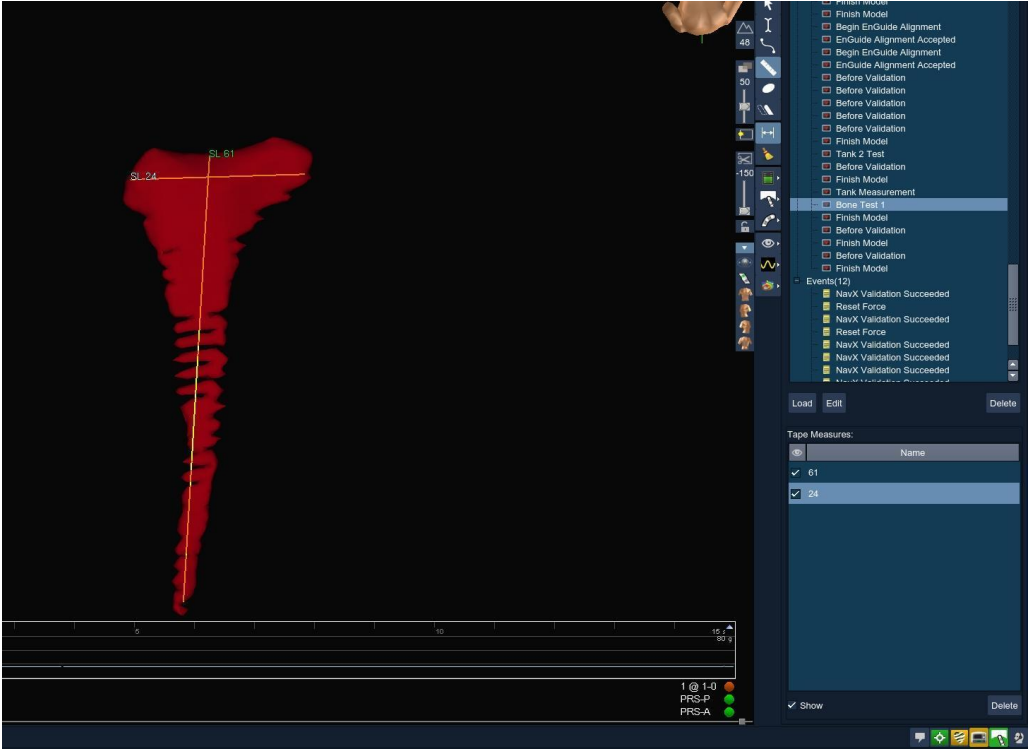
Cal Poly Biomedical Engineering	Lab Section:	Assignment #	Title: End Pane (Length)	Drwn. By: Bosung Kim
BMED 592 - Summer 2021	Dwg. #:	Nxt Asb:	Date: 7/23/2021	Chkd. By:

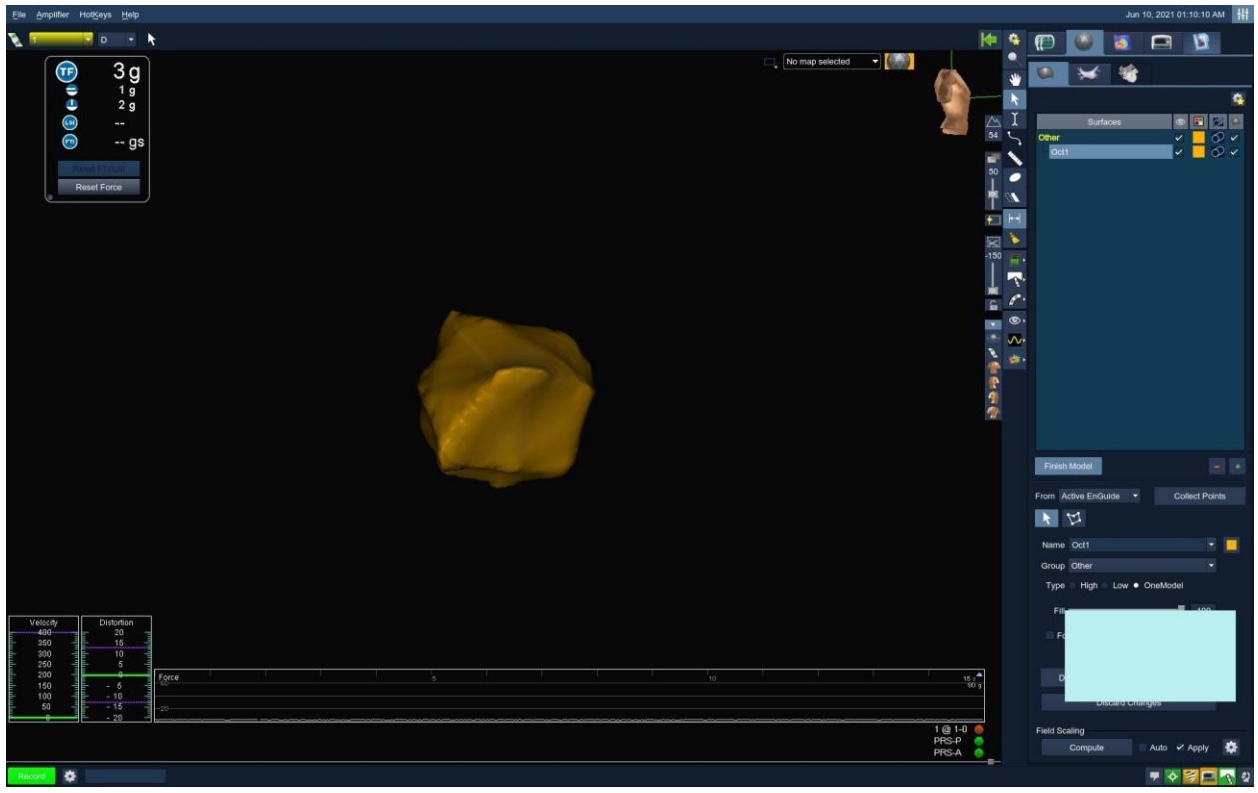
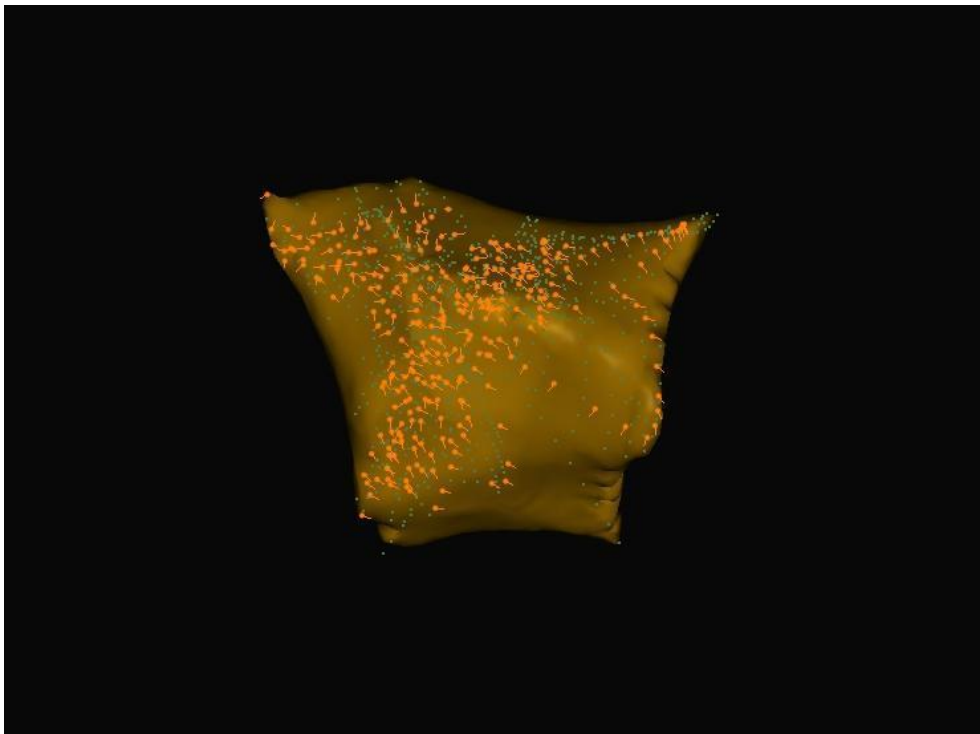
Appendix D: Test data











File Amplifier HotKeys Help Jun 10, 2021 01:10:10 AM

3g
1g
2g
--gs
Reset Force

No map selected

Velocity	Distortion
400	20
300	15
200	10
100	5
50	2

Force

Field Scaling
Compute Auto Apply

Surfaces
Other
Oct1

Finish Model

From Active EnGuide Collect Points

Name Oct1

Group Other

Type High Low OneModel

Field Scaling
Compute Auto Apply

Appendix E: Operation Manuals

Integration For Mapping Protocol

System Components:

- EnSite Amplifier
- Fiber Optic Cables
- EnSite Precision Link, Sensor Enabled, NavLink Module
- TactiSys Quartz
- EnSite Precision Field Frame and bracket
- Field Frame cable
- Display Workstation
- Monitor Boom (Patient Monitors)

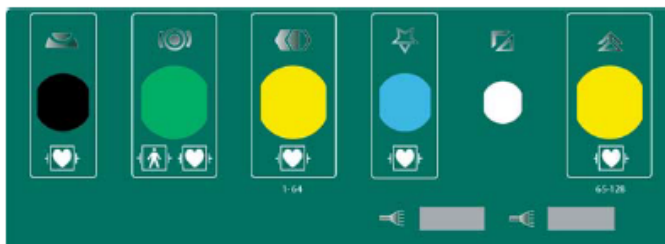
External Components:

- TactiCath SE ablation catheter
- EnSite Precision or Velocity electrode kit
- Patient Reference Sensors

*Note: This protocol was designed to be used when collecting data points with TactiCath SE catheters in conjunction with the EnSite Precision Link, Sensor Enabled, NavLink Module. For mapping with the CathLink Module and diagnostic catheters, please refer to the Instructions for Use.

1. Turn on the EnSite Amplifier and allow 30 minutes for it to warm up
2. Connect the EnSite Precision Cardiac Mapping System component cables to the EnSite Amplifier

Icon	Connector Color	Function
	Black	GenConnect
	Green	NavLink™ Module
	Yellow	CathLink™ Module or RecordConnect catheter
	Blue	ECG or RecordConnect ECG
	White	ArrayLink™ Data Module
	Yellow	ArrayLink™ Module, CathLink™ Module, or RecordConnect Catheter



3. Place the system reference electrode on the tank (see figure below for positioning), then connect the electrode lead to the NavLink Module
4. Place EnSite Precision surface electrodes on the tank (see below for positioning), then connect all electrode leads to the NavLink Module
5. Turn on the Display Workstation
6. Log into the EnSite Precision Cardiac Mapping System
7. Start a new EnSite NavX Navigation and Visualization Technology Study
 - a. Click **New Study** from the Clinical Menu
 - b. Click **New Patient**
 - c. Enter weight of the sample
 - i. The rest of the information fields must be entered before study ends and can be filled in with user's information

- d. Click **Next** to display Study Setup screen
 - e. Select **EnSite NavX**
 - f. Enter study information
 - g. Select appropriate Recording System
 - h. Click **Begin Study**
8. Connect EP catheters to the appropriate modules
 - a. Ablation catheters connected to the TactiSys Quartz and the Precision Link
 - b. Diagnostic catheters connected to the CathLink Module
9. Perform an EnSite Precision Module Functional Check
 - a. Ensure the Patient Reference Sensor (PRS) are connected to each of the two REF ports on the module
 - b. Position each PRS at their appropriate location on the tank
 - i. The indicators turn green to confirm that the PRS is inside the detection area of the Field Frame
 - ii. Verify this in the NavX SE page of the setup tab
10. Perform validation
 - a. Insert the Data Module connection into the NavLink module
 - i. The Data Module is incorporated in the EnSite Precision left leg surface electrode
 - b. Click **Amplifier** drop down menu located at top left of the screen
 - c. Click **Validate** at the bottom of the list to begin the validation process. When complete, a message appears in the lower right side of the screen
 - d. If validation fails, check connections then revalidate from the menu bar by selecting **Amplifier > Validate**

11. Perform EnSite NavX Navigation and Visualization Technology setup

- a. Select the Setup tab
 - i. Open up the Catheter Setup page
 - ii. In between the two virtual CathLink modules, locate the GeoConnect terminals
 - iii. Drag the pins to the appropriate pin ports on the module
- b. Select the model tab
 - i. Open the model page and add new model using the + button
 - ii. Use the **Name** drop-down to select an existing name or type the desired name
 - iii. Set the following parameters in the model control panel
 1. From: Active EnGuide
 2. Group: Left or Right
 3. Type: OneModel
 4. Fill: 35-100 (75 preferred)
 5. Leave Force Unchecked
 6. Points: None
 7. Field Scaling: select both Auto and Apply checkboxes
 8. Under the Field Scaling settings wheel on the bottom right, select NavX
SE
- c. In the Filter Controls section in the Waveforms display area, adjust the bipolar and unipolar signals to reduce the amount of noise read by the system.

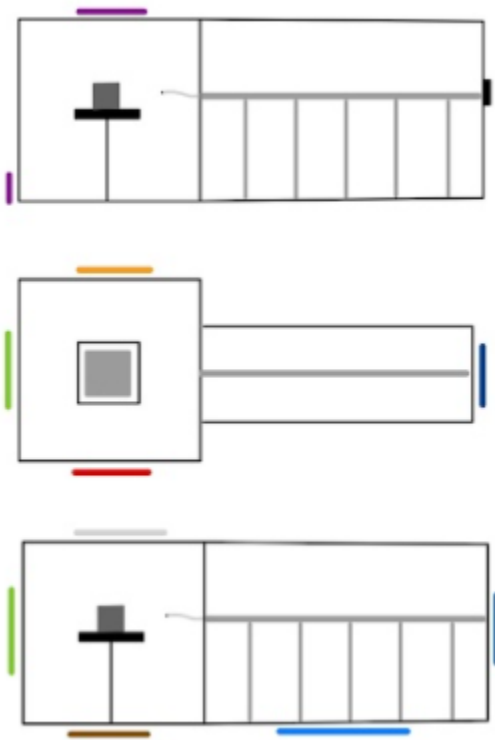
12. Create a model

- a. Set the catheter inside the object of interest
- b. In the model control panel click **Collect Points** to begin collecting points.

- c. Drag the catheter along the walls of the object and throughout the interior to create a surface, retouching each location multiple times
- d. Before removing the catheter, press **Stop Collecting Points** to stop collecting points
- e. Click **Finish Model** when the model creation is complete. Otherwise, repeat all steps in parts 11b, 11c and 12 for all additional surfaces

13. End Study

- a. Select **File > End Study**
- b. Fill out any required fields



Top image: Side View

Bottom image: Top View

Patch Placement:

PRS Patches (purple)

EnSite System Reference Electrode (light blue)

Neck (green)

Chest (light grey)

Back (brown)

Right (red)

Left (orange)

Left Leg (blue)

Protocol for adding EP catheters with RecordConnect

- Before adding catheters to the study ensure that the appropriate ReadyConnect has been specified for the study.
 - To select a different CIM, from the menu bar select **Amplifier > Settings > RecordConnect** then click the appropriate checkbox for the recording system being used
- Depending on the catheter you are using, add by one of the following methods

Selecting a Catheter from the Catheter Catalog

1. Click **Catheter Catalog**
2. In the new window, choose the desired catheter from the catalog list
3. Click **Add New** at the lower right of the catalog window
4. Choose remaining catheters or close the catalog window with the **Close** button at the lower right corner of the window

Defining a Catheter

1. Click the + button beneath the Catheter List
2. Enter catheter name
3. Select a color for the catheter body. The color of the waveforms for the catheters defaults to the color selected for the catheter body
4. Specify the catheter properties: **number of electrodes, catheter diameter, distal length, electrode length, electrode spacing**. When specifying the number of electrodes, the electrodes will be assigned to consecutive Input Channels starting with the distal electrode assigned to the first available channel
5. From the **Polarity** drop-down menu, specify whether signals should be collected from paired bipoles, all possible bipoles, or all possible unipoles
6. Select the filters using the filter controls
7. If using for multiple sessions, click **Add to Catalog**

Protocol for adding EP catheters with RecordConnect

- Before adding catheters to the study ensure that the appropriate ReadyConnect has been specified for the study.
 - To select a different CIM, from the menu bar select **Amplifier > Settings > RecordConnect** then click the appropriate checkbox for the recording system being used
- Depending on the catheter you are using, add by one of the following methods

Selecting a Catheter from the Catheter Catalog

1. Click **Catheter Catalog**
2. In the new window, choose the desired catheter from the catalog list
3. Click **Add New** at the lower right of the catalog window
4. Choose remaining catheters or close the catalog window with the **Close** button at the lower right corner of the window

Defining a Catheter

1. Click the + button beneath the Catheter List
2. Enter catheter name
3. Select a color for the catheter body. The color of the waveforms for the catheters defaults to the color selected for the catheter body
4. Specify the catheter properties: **number of electrodes, catheter diameter, distal length, electrode length, electrode spacing**. When specifying the number of electrodes, the electrodes will be assigned to consecutive Input Channels starting with the distal electrode assigned to the first available channel
5. From the **Polarity** drop-down menu, specify whether signals should be collected from paired bipoles, all possible bipoles, or all possible unipoles
6. Select the filters using the filter controls
7. If using for multiple sessions, click **Add to Catalog**

Appendix F: Testing Protocol

Leak Test Protocol

1. Place the chamber inside the bathtub, make sure the base is parallel to the bathtub.
2. Fill the tank with saline solution to the desired amount in **cups** (18, 22 , 26, 32,36)
3. Let sit for 10 minutes. Observe for leaks or cracks
4. Record location for leaks
5. Remove water from chamber
6. Let chamber dry naturally or wipe down all moisture with a towel
7. Apply rubber sealant to specific locations
8. Repeat for remaining sample amounts

Pressure Test

1. Horizontal Force test
 - a. Place the tank on its side (one of the panes are on the ground)
 - b. Place weight until sign of fracture in the epoxy/glue
 - c. Record Weight
2. Vertical Test
 - a. Place a wide sheet of cardboard on top of the tank
 - b. On top of the cardboard put weight until sign of fracture in the epoxy/glue
3. Calculate Volumetric pressure/ Weight by water on tank

Saline Validation test

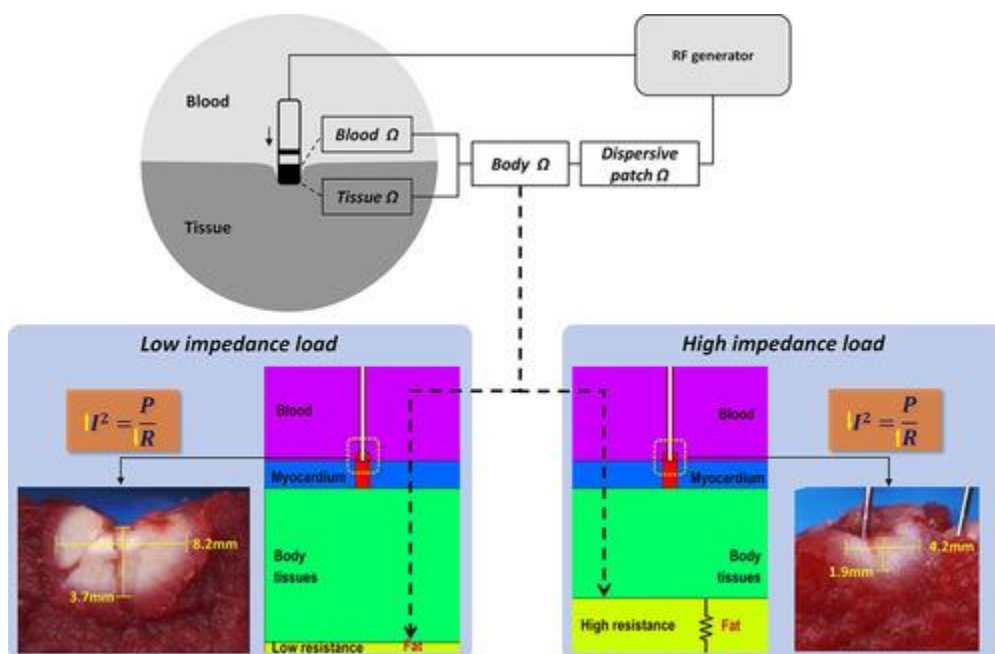
1. Pour saline solution in to the tank
2. Place two electrodes on a stable surface in the saline solution
3. Measure the impedance between the two electrodes

4. Add salt or water until the desired impedance of 131-180 ohms is achieved

*Note: impedance is important if we decide to perform ablation for our spring experimental design

1. Perform the validation portion of the Integration for Mapping protocol ensure that all equipment is setup properly and integration is established
2. Using the saline solution protocol, create a batch with the desired salinity and pour into the tank
 - a. If a certain solution temperature is required, place the heating element in the tank until the temperate is attained
3. Place the object of interest in working area of tank on top of a material that is either conductive or not resistive to a passing current
 - a. Acrylic or glass prefered
4. Place the catheters in the long portion of the tank and rest them hanging off the ledge inside the solution ensuring there is no contact with the tips of the catheter
5. Perform the EnSite NavX Navigation and Visualization Technology setup from the Integration for Mapping protocol
6. Perform the Create a Model portion of the Integration for Mapping protocol to collect data points that will create the geometry of the item
7. Using the trim tool, cut out any unnecessary data points that hinder the model
8. Once the final model is created, use the measure tool to gather the dimensions of the model created by the system
9. Compare the generated measurements to the physical measurements

10. Repeat 5-9 for all remaining objects



Appendix G: Manufacturing process instructions

Cutting Acrylic

1. Measure out acrylic sheets to the dimensions of the design
2. Using the table saw miter saw
 - a. Ask the Mustang 60 Tech Shop for assistance, rent out blades
 - b. For straight cuts, keep the blade at 90 degrees
 - c. Place the material that is needed to be cut in front of the blade with the correct measurement using the ruler on the table.
 - d. Power on the device (the blade should be rotating)
 - e. Push the material (acrylic) with your hand or a pusher slowly
 - f. Once the cut is made power off the device

Laser Cutting Acrylic

- a. Using the Solidworks drawings, create drawings from faces and export as drx files.
- b. Email the drx file or save the files on a flash drive
- c. Set up the laser cutting machine (Ask machine shop tech if help is needed)
 - i. Set up z-axis height
 - ii. Turn on air vent/ power
- d. Open Adobe illustrator on the PC connected to the laser cutting machine
- e. Open the drawing files and position onto the 18" x 32" file

- f. Print the file, and send through the laser cutting machine and observe the process

Assembly of Acrylic Panes

- a. Have the gorilla epoxy ready at hand
- b. Once the epoxy is opened, squeeze both liquid into a “tray” and stir for “20 seconds”
- c. You would start to pick up a distinct smell once the chemical begins working and have about 5 mins to apply the solution on to the surfaces
- d. Apply the epoxy onto the sides of the acrylic panes and stick them close.
- e. While letting them dry, apply masking tape to help the pieces hold its place

Saline Solution Manufacturing Process

Materials:

Tap Water

Table salt or fine sea salt (iodine- free)

Pot or microwave-safe bowl with a lid

Clean Jar

Measuring cup

Teaspoon

Baking Soda (optional)

Stovetop method

1. Boil 2 cups of water covered for 15 minutes

2. Allow to cool to room temperature
3. Add 1 teaspoon of salt
4. Add 1 pinch of baking soda
5. Stir until dissolved
6. Refrigerate in airtight container for up to 24 hrs
7. Add 2 cups of water to a microwave-safe container
8. Mix in 1 teaspoon of salt'
9. Microwave, covered, for 1 to 2 minutes
10. Allow to cool.
11. Place in a clean jar
12. Refrigerate for up to 24hours

For a more sterile and long-lasting version, we use distilled water.

*Throw away if cloudy or dirty

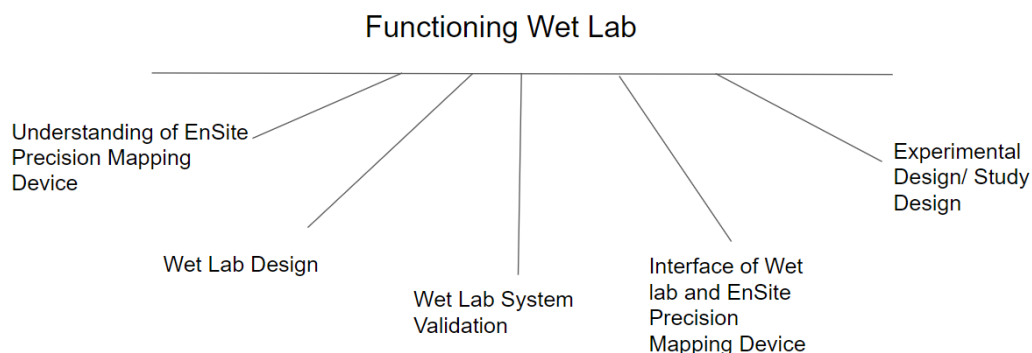
*Make sure to put 8 teaspoons of table salt to 1 gallon of distilled water

*Can refrigerate for up to 1 month.

Appendix H: Core Customer Charts

Success Criteria

Includes	Does Not Include
<ul style="list-style-type: none"> ● A functioning wet lab for mapping ● Integration between wet lab and EnSite Precision Mapping System ● Accurate mapping results produced from tests done in the wet lab ● Yield accurate results from experimental study 	<ul style="list-style-type: none"> ● A functioning wet lab for catheter ablations and other non-mapping procedures ● Alterations to existing catheters and mapping patches ● Developing the wet lab to be functional with other mapping systems



We will be developing a functioning wet lab that will be fully integrated with Abbott's EnSite Precision Mapping System which will be utilized for future testing of products, validation of student projects, and performing student labs. This project and subsequent studies will cost approximately \$500 and will be completed by June 2021. To successfully complete this project, all the main deliverables in the web above must be completed while achieving accurate napping geometry, and yielding accurate results from the experimental study.

Flexibility Matrix

	Least	Moderate	Most
Scope	X		
Schedule		X	
Resources			X

At the beginning of the quarter we established that the scope of the project was the least flexible, the resources were the most flexible and the schedule was in-between those aspects. At the moment, the flexibility remains the same but if we endure more restrictions due to COVID, this chart may shift because our schedule will become more defined.

Ensite Precision Mapping Device

Includes	Does Not Include
<ul style="list-style-type: none"> Understanding the function/capabilities of the device Risk/ Safety Hazard of Device Functional Device Set-up 	<ul style="list-style-type: none"> Improvement on Software & Hardware of the device Maintenance of the Device Device Installation

Wet Lab Design

Includes	Does Not Include
<ul style="list-style-type: none"> Cost of Wet Lab Knowledge of functionality of Wet Lab Wet Lab prototyping Literature Survey of Existing Wet Labs Material/ Ordering Parts 	<ul style="list-style-type: none"> Developing the wet lab to be functional with other mapping systems Aesthetics Currents (electricity) in the saline solution

Wet Lab System Validation

Includes	Does Not Include
<ul style="list-style-type: none"> • Capability of allowing images to be created • Temperature Control • Saline Environment (no leak) • Device Functionality • Device specification testing 	<ul style="list-style-type: none"> • Being functional with Abbot's Mapping Device • Not worried about if the wet lab produces accurate images or data

Interface of Wet lab and EnSite Precision Mapping Device

Includes	Does Not Include
<ul style="list-style-type: none"> • Produce an Image on Abbott's device • Accurate measurement/ mapping performed in wet lab • Wet lab is easily interfaced with the Abbot system 	<ul style="list-style-type: none"> • Other systems or interfaces • Study/Design for validation of functions of the wet Lab and the Device


Experimental Design/Study Design

Includes	Does Not Include
<ul style="list-style-type: none"> • Demonstrates integration is accurate • Provides insight on limitations of wet lab testing • Design a study involving the wet lab to validate the accuracy of the "mapping", and provide insight into the capabilities of the wet lab. 	<ul style="list-style-type: none"> • Developing and validating new catheters or mapping products


Risk Assessment

Potential Issue	Alternative Solutions
Inability of Abbott engineers to assist in-person	Set up cameras around the system to allow virtual assistance
Testing Errors	Perform tests multiple times under various conditions
System Malfunction	Consult with Abbott engineers who specialize in the design of the system
Cal Poly COVID Regulation for In-Person Attendance	Entry Log, Shared Calendar/Schedule, Social Distancing, Sanitation

Appendix I: Penta Chart




Penta Chart



Abbott Lab Instrumentation Validation and Wet Lab Design; Brandon Mukai, Bosung Josh Kim


Status Quo



- Current lab setup does not simulate physiological environments
- In order to test new products and validate future projects, wet lab must simulate physiological environments and integration must yield accurate results

Research/Development Approach

Hypothesis: It is feasible to create a wet lab that integrates with the EnSite Precision Mapping System to yield accurate test results.

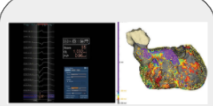


Approach: After validating the functionality of the mapping system, a wet lab will be designed to integrate with the system. The lab will be tested with various experimental studies that will determine the functionality and accuracy of the integration.

Risk Assessment:


- Inability of Abbott Engineers to assist in-person
- Testing errors
- System malfunction
- Cal Poly COVID Regulation for In-Person Attendance

Quantitative Impact



- Mapping with catheters will be >95% accurate (subject to change) when testing with wet lab

New Insights



- Sterile tank with saline solution and thermoregulation can simulate physiological environments
- Wet lab will allow accurate integration with system

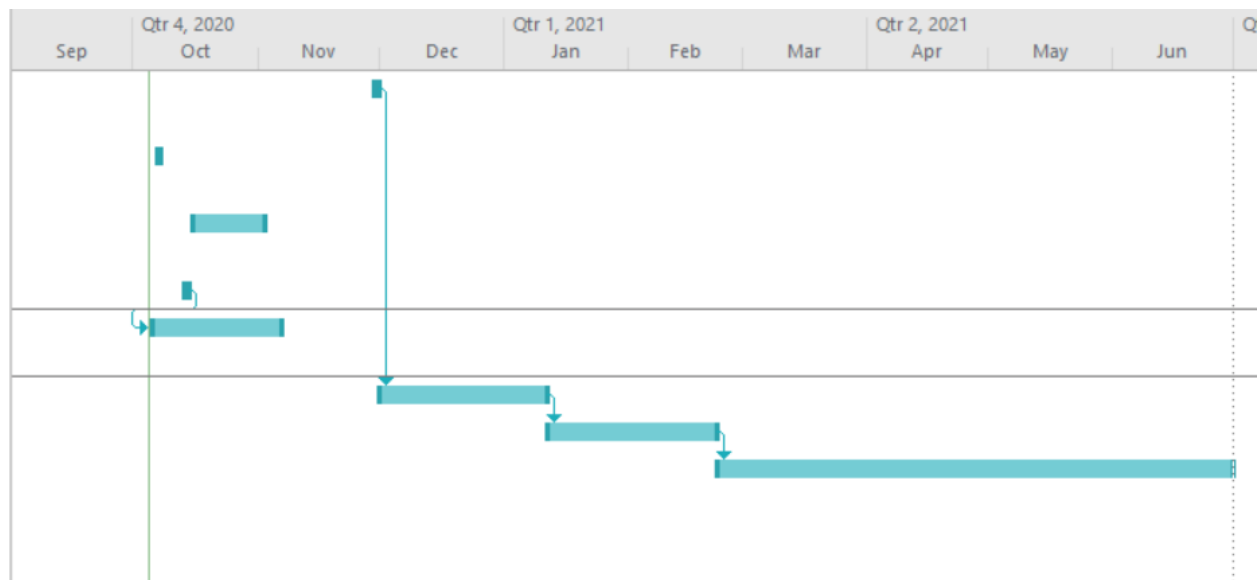
End-Of Project Goal

After validating the accuracy of the integration, the wet lab will be able to test future products, validate student projects, and allow students to perform laboratory experiments.

- Wet lab can be altered and upgraded to perform other procedures such as catheter ablations
- Future student/faculty products can be validated using the wet lab
- Faculty and industry personnel can use lab for demonstrations

BMED 591-01 A functional and accurate integration between the wet lab and the system will allow next generation students and faculty to test their products in a physiologically accurate environment.

As mentioned above, the goal is to create a functioning wet lab that integrates with Abbott’s mapping system to yield accurate test results. There is not currently a wet lab available in the St. Jude lab that simulates physiological environments for testing so we will be incorporating that into our build. This will be done with a saline solution that represents the



★	BMED 599 Winter Quarter	54 days?	Mon 1/4/21	Mon 3/22/21	
★	Research of Existing Wet Lab designs	15 days	Sat 1/2/21	Fri 1/22/21	
★	Meeting with Dr. Porterfield	1 day	Mon 1/11/21	Mon 1/11/21	
★	Meeting With Dr. Heylman	1 day	Wed 1/13/21	Wed 1/13/21	
★	Contact Abbott Engineer	14 days	Wed 1/6/21	Tue 1/26/21	27
★	Prototype Development	10 days	Tue 1/26/21	Mon 2/8/21	27
★	Meeting with Dr. Porterfield	1 day	Thu 2/4/21	Thu 2/4/21	
★	Order materials	1 day	Tue 2/9/21	Tue 2/9/21	31,30
★	Meet with Dr. Heylman	1 day	Wed 2/10/21	Wed 2/10/21	
★	Build Prototype	5 days	Wed 2/10/21	Wed 2/17/21	33
★	Prototype Adjustments	1 wk	Wed 2/17/21	Tue 2/23/21	
★	Tank Test Validation	3 days	Thu 2/25/21	Mon 3/1/21	
★	Project Plan Presentation	2 days	Fri 3/5/21	Sun 3/7/21	
★	Report	2 wks	Tue 2/23/21	Sun 3/7/21	
★	Progress Presentation	4 days	Wed 3/3/21	Sun 3/7/21	

✦	✦	BMED 592 Spring Quarter	56 days?	Mon 3/29/21	Sun 6/13/21		
✦		Project Status Update Memo	1 wk	Tue 3/30/21	Mon 4/5/21		
✦		Project Status Update Memo #2	1 wk	Tue 4/20/21	Mon 4/26/21		
✦		Project Progress Report	1 mon	Tue 4/27/21	Mon 5/24/21		
✦		Individual Report	1 mon	Tue 4/27/21	Mon 5/24/21		
✦		592 Report detailed outline	1 mon	Tue 4/27/21	Mon 5/24/21		
✦		Project Progress Presentation	2 wks	Tue 5/18/21	Mon 5/31/21		
✦		Lab notebook	2 mons	Tue 4/6/21	Mon 5/31/21		
✦		Tank Integration	26 days	Fri 5/7/21	Fri 6/11/21		
✦		Prototype Manufacturing	16 days	Fri 5/21/21	Fri 6/11/21		

Appendix K: Budget

Proposed:

Item Description	Product Number	Purpose	Associated Task	Planned					Actual			
				Unit	Quantity	Cost/Unit	Total Cost	Notes	Quantity	Cost/Unit	Total Cost	Notes
2"x4"x96" Prime Whitewood Stud	161640	Structure for table		EA	4	\$5.85	\$23.40	Home Depot				
Gorilla 8 oz Wood Glue	62000	Building of table		EA	1	\$3.97	\$3.97	Home Depot				
#8x2-1/2" Phillips Bulge-Head Coarse Thread Sharp Point Polymer Coated Exterior Screws	134228	Building of table		EA	1	\$8.97	\$8.97	Home Depot				
3M Pro Grade Precision 9"x11" 80,150,220 Assorted Grits Advanced Sanding Sheets	26000PGP-6	Building of table		EA	1	\$8.97	\$8.97	Home Depot				
PlexiGlass 24 by 24	SPLEXICL187-24X	Building IVT Chamber		EA	2	\$23.44	\$46.88	Professional Plastics				
Painter's Tape	2090-48CP	Building Chamber		EA	1	\$6.58	\$6.58	Home Depot				
Silicone Sealant	GE012A 12C	Building Chamber		EA	1	\$5.37	\$5.37	Home Depot				
Sand Paper	Owned						\$0.00					
Digital Scale	Owned						\$0.00					
sousvide machine		tempertaure control		EA	1	\$61.99	\$61.99	Amazo 13.77 x 2.16 x 2.16 inches				
							\$0.00					
Total							\$166.13					

Final:

